IEEE Access
Multidisciplinary | Rapid Review | Open Access Journal

Received March 20, 2018, accepted April 15, 2018, date of publication April 27, 2018, date of current version May 24, 2018.

Digital Object Identifier 10.1109/ACCESS.2018.2830801

Performance Analysis of Multi-Antenna Multiuser Hybrid Satellite-Terrestrial Relay Systems for Mobile Services Delivery

VINAY BANKEY[1], (Student Member, IEEE), PRABHAT K. UPADHYAY[1], (Senior Member, IEEE), DANIEL BENEVIDES DA COSTA[2], (Senior Member, IEEE), PETROS S. BITHAS[3], (Member, IEEE), ATHANASIOS G. KANATAS[3], (Senior Member, IEEE), AND UGO SILVA DIAS[4], (Senior Member, IEEE)

[1]Discipline of Electrical Engineering, Indian Institute of Technology Indore, Indore 453552, India
[2]Department of Computer Engineering, Federal University of Ceará, Sobral 62010-560, Brazil
[3]Department of Digital Systems, University of Piraeus, Piraeus 185 34, Greece
[4]Department of Electrical Engineering, University of Brasília, Brasília 70910-900, Brazil

Corresponding author: Vinay Bankey (phd1501202007@iiti.ac.in)

The work of D. B. da Costa was supported in part by CNPq under Grant 302863/2017-6 and in part by FUNCAP, Edital PRONEM 01/2016. The work of U. S. Dias was supported by the Ministry of Justice, Government of Brazil, under Grant TED-FUB/UnB-SENACON/MJ 001/2015.

ABSTRACT Satellite communication systems need to be integrated with emerging cooperative relaying techniques to provide seamless connectivity and high-speed broadband access for mobile users in future wireless networks. In this paper, we study a multi-antenna multiuser hybrid satellite-terrestrial relay network (HSTRN) employing opportunistic user scheduling with outdated channel state information (CSI) and amplify-and-forward relaying with co-channel interference (CCI). By adopting Shadowed-Rician fading for satellite links and Nakagami-*m* fading for terrestrial links, we derive novel and accurate expressions for outage probability and ergodic capacity of the proposed HSTRN, and further examine its achievable diversity order. More importantly, we conduct the performance analysis by taking both uncorrelated and correlated Shadowed-Rician fading channels into account and show that the antenna correlation at the satellite does not affect the overall system diversity order. Our derived analytical expressions provide efficient tools to characterize the impact of CCI, outdated CSI, and antenna correlation on the system performance of HSTRN with an arbitrary number of satellite antennas, number of interferers, number of users, and integer values of the per-hop fading severity parameters. Our results provide useful guidelines in the design of futuristic HSTRNs for satellite mobile communications.

INDEX TERMS Amplify-and-forward relaying, co-channel interference, ergodic capacity, hybrid satellite-terrestrial systems, multiuser scheduling, outage probability, Shadowed-Rician fading.

I. INTRODUCTION

The growing demand for high data rates and high-fidelity services anytime and anywhere have stimulated the deployment of satellite mobile communications in the fifth generation (5G) era. A hybrid satellite-terrestrial network has been incorporated in Digital Video Broadcasting (DVB) system which provides Satellite services to Handheld devices (SH) by making use of a geostationary (GEO) satellite operating at S (2/4 GHz) band, leading to a high performance new generation standard, known as DVB-SH [1]. The transmission systems using such standards have been proposed to provide multimedia services to a variety of mobile terminals, along with a complementary ground network consisting of terrestrial repeaters fed by a broadcast distribution network of various kinds (e.g., DVB-S2). The target terminals may include handheld (PDAs, mobile phones, etc.), vehicle-mounted, and nomadic (laptops, palmtops, etc.) devices.

Recently, researchers have envisaged the integration of satellite and terrestrial systems to form a hybrid satellite-terrestrial relay network (HSTRN) model [2]–[4], which basically implants terrestrial relay cooperation to satellite mobile communications [5]. Such HSTRN can provide broadcast/multicast services and uninterrupted coverage to portable and mobile users. It enhances indoor coverage and retains

service availability, especially in highly shadowed regions like shopping malls, tunnels, etc., where the users do not have line-of-sight (LOS) communication with the satellite due to masking effect. While many works have analyzed the performance of HSTRN using amplify-and-forward (AF) [6]–[10] and decode-and-forward (DF) relaying [11]–[13], they have focussed on a single-user scenario. Multiuser relay network is a promising architecture for future mobile communication systems, wherein a relay can assist the communication between a source and multiple destinations/users [14]. Such architecture has been adopted in a number of standards like IEEE 802.11s and IEEE 802.16j [15]. The HSTRN has also been extended to a multiuser scenario [16], [17] since the futuristic 5G mobile systems need to provide high throughput services to a large number of terrestrial users. Specifically, in [16], a multiuser HSTRN has been studied with opportunistic user scheduling to exploit multiuser diversity. In [17], a multi-user multi-relay architecture for HSTRN has been explored. However, these works have assumed the knowledge of perfect channel state information (CSI) to facilitate the user selection process. In practice, the CSI for user selection may be outdated due to various reasons such as feedback delay, mobility, etc. Further, with dense frequency reuse in wireless networks, the HSTRN is prone to co-channel interference (CCI). Although few works [8]–[10], [13] have considered the impact of CCI on the performance of HSTRN, they are limited to the single user scenarios. Toward this end, in a preliminary work [18], the performance of an AF-based multiuser HSTRN has been investigated by employing opportunistic user scheduling in the presence of outdated CSI and CCI at the relay.

On another front, significant research attention has been directed towards deploying multiple-input multiple-output (MIMO) technology with satellite communication systems to achieve performance gains with multiple antennas [19]–[21]. Indeed, the channel and propagation characteristics of satellite links are different from the terrestrial links and thereby potential MIMO exploitation in satellite communication is of primary concern. The main difference lies in the LOS characterization of satellite channels and the lack of scatterers around the satellite. This may result into a strong LOS and a high channel correlation due to insufficient antenna separation and sparse scattering environment at the transmitting satellite. As such, the multipath fading effects over the spatial dimension may get subsided and the potential benefits of MIMO could not be fully exploited in such scenario. With this view point, few recent works have considered correlated fading channels over satellite links, and exploited beamforming [22], [23] and space-time coding [24], respectively, in dual-hop and single-hop land mobile satellite systems. Besides these, majority of the works on MIMO satellite communications (e.g., see [25]–[28] and references therein) have adopted independent and identically distributed (i.i.d.) assumptions for the pertaining multiple channels. In particular, the authors in [26] have established the MIMO channel model of Ka-band satellite-earth link and evaluated its error performance using i.i.d. entries. They have pointed out that the technology of artificially disturbing channel can make it a way for producing the i.i.d. channel fading matrix for the satellite MIMO communication. In fact, the theoretical studies on such topics have recently begun with a main focus on determining the system performance limits. Moreover, in the most recent literature [29]–[31], it has been emphasized that the satellite communication system must be integrated with the terrestrial network to fulfil the requirements of 5G wireless network. Thereby, it is important to evaluate the performance of multiuser HSTRNs with MIMO configuration in realistic operating conditions.

In contrast to the previous works, in this paper, we study a more generalized HSTRN architecture[1] by configuring with multiple terrestrial users, multiple co-channel interferers at the AF relay, and multiple antennas at the satellite and users/destinations. Specifically, we employ MRT and MRC based transmit and receive beamforming at the satellite and land mobile users respectively. Considering mobility of land users, we employ user scheduling with outdated CSI over Nakagami-m fading channels of pertinent links. Moreover, by adopting both i.i.d. and correlated Shadowed-Rician fading[2] channels for satellite links,[3] we conduct a comprehensive performance analysis of the proposed HSTRN in terms of outage probability (OP) and ergodic capacity (EC) in the presence of outdated CSI and CCI with arbitrary number of antennas, number of interferers, number of users, and arbitrary integer values of the fading severity parameters over the two hops. Such investigation is important to understand the achievable performance of HSTRN for its potential deploy-

[1]This corresponds to a downlink multiuser HSTRN, where a source satellite communicates with multiple users with the assistance of a single-antenna relay at the ground. The assumption of single-antenna relay is reasonable since, in many practical scenarios, a low power repeater could be located at the rooftop of a building or on an unmanned aerial vehicle (UAV) in order to achieve coverage in urban areas where the direct satellite signal power is poor. In such scenarios, it is very likely that limited scattering phenomena will be expected due to the absence of local scatterers around the communication antennas and thus the adoption of diversity techniques will not offer any important gain. Moreover, in various scenarios, the relay is not able to support sophisticated transceiving techniques, e.g., maximal-ratio transmission (MRT) and maximal-ratio combining (MRC), due to space/energy constraints that are imposed by the use case assumed. For example, if the relay is mounted in an aerial platform, it is meaningless to include multiple antennas in such a limited available space with so restricted energy constraints. It should be noted that various works in the past have also assumed single-antenna relay communication scenarios in similar system models e.g., [28], [32]–[35].

[2]The Shadowed-Rician channel model, as defined in [36], describes accurately the land mobile satellite communication channel, where a random LOS component follows Nakagami-m distribution with $0 \leq m \leq \infty$, while the multipath component follows the Rician fading. This model is widely adopted in literature [6] and [27] for the performance analysis of hybrid satellite-terrestrial systems since it offers less computational burden as compared to other models like Loo's model [37].

[3]Herein, we assume perfect CSI acquisition with negligible Doppler spread over the satellite-relay links by considering a GEO satellite and a fixed location of the terrestrial relay. Albeit, in [38], authors have studied such problems of channel estimation and associated imperfection for a basic HSTRN, the research in this domain is in still infancy and is a topic for future investigation. Nevertheless, our presented results will serve as a benchmark of system performance for the multi-antenna multiuser HSTRN.

ment in futuristic wireless systems. The major contributions of this paper can be summarized as follows:

- We study a MIMO based multiuser HSTRN employing AF relaying in the presence of CCI and opportunistic scheduling of terrestrial users in the presence of outdated CSI, under Shadowed-Rician faded satellite links and Nakagami-*m* faded terrestrial links. This is a more generalized, realistic and complicated set-up as compared with existing ones that considered either single-user systems [22]–[28] or single-antenna systems [16], [18]. Although [17] considered a multi-antenna satellite, it is resorted to the ideal case of i.i.d. links, perfect CSI, and no CCI.
- By considering both i.i.d. and correlated Shadowed-Rician fading scenarios at satellite, we derive accurate OP expressions for the proposed HSTRN over generalized hybrid channels. This is in contrast to that presented in [28] where an upper bound OP expression has been derived for much simpler and ideal case of single-user HSTRN with i.i.d. Shadowed-Rician satellite links and Rayleigh fading terrestrial links, and it also does not always lead to tight results.
- We further deduce asymptotic OP expressions in the high signal-to-noise ratio (SNR) regime to evaluate the diversity performance of the considered HSTRN and illustrate that the achievable diversity order would not get affected with antenna correlation at the satellite.
- We also derive novel and accurate expressions for the EC of the proposed HSTRN under both i.i.d. and correlated Shadowed-Rician satellite links and Nakagami-*m* fading terrestrial links. Our numerical and simulation results highlight the impact of various key parameters on the system performance of HSTRN.

The rest of this paper is organized as follows. In Section II, we explain system model for a multi-antenna multiuser HSTRN. We present the performance analysis of proposed HSTRN by considering uncorrelated Shadowed-Rician fading channels in Section III. Subsequently, we conduct the system performance analysis under correlated Shadowed-Rician fading scenario in Section IV. Section V presents the numerical and simulation results, and finally, the conclusions are drawn in Section VI.

Notations: $E[\cdot]$ represents the expectation and $\mathcal{CN}(\mu, \sigma^2)$ denotes complex normal distribution with mean μ and variance σ^2. $f_X(\cdot)$ and $F_X(\cdot)$ represent the probability density function (PDF) and cumulative distribution function (CDF) of a random variable (RV) X, respectively. $||\cdot||_F$ is Frobenius norm and $(\cdot)^\dagger$ denotes conjugate transpose. $\mathbf{I}$ represents the identity matrix. $\mathcal{C}_\iota^\ell = \frac{\ell!}{(\ell-\iota)!\iota!}$ is binomial coefficient. $\Upsilon(\cdot,\cdot)$ and $\Gamma(\cdot)$ represent, respectively, the lower incomplete and the complete gamma functions [49, eq. (8.350)].

II. SYSTEM MODEL

As shown in Fig. 1, we consider a multi-antenna multiuser HSTRN wherein a GEO satellite source S communicates with

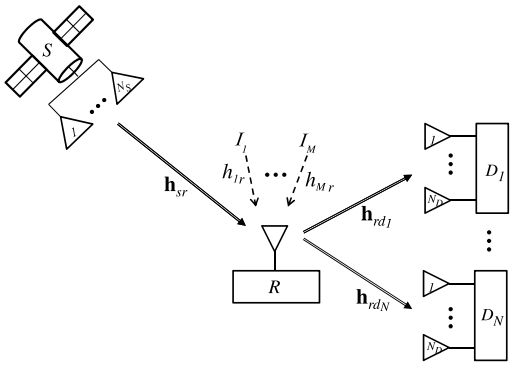

FIGURE 1. HSTRN model with MIMO configuration.

N terrestrial destinations $\{D_n\}_{n=1}^N$ via a terrestrial AF relay R. The satellite S and all destinations D_n are equipped with N_s and N_d antennas, respectively, while the relay R is equipped with a single antenna. Further, we consider that the relay node is inflicted by M co-channel interferers $\{I_i\}_{i=1}^M$ and each user is inflicted by the additive white Gaussian noise (AWGN). This is a commonly adopted scenario with respect to frequency division relaying systems [11], [13], [39] wherein the relay and user nodes experience different interference patterns.[4] Due to shadowing effects, the direct links between the satellite and the terrestrial users are not available. These direct links could be masked in certain scenarios such as heavy shadowing, obstacles in the environment, users moving to tunnels, indoor users, etc. We denote $\mathbf{h}_{sr}$ as the $N_s \times 1$ Shadowed-Rician channel vector between N_s antennas at S and R. Likewise, $\mathbf{h}_{rd_n}$ represents the $N_d \times 1$ Nakagami-*m* channel vector between the R and the N_d antennas at nth destination D_n. Whereas, h_{ir} denotes the channel coefficient of the link between ith interferer and relay. We assume that the fading coefficients $\{h_{ir}\}_{i=1}^M$ are independent and non-identically distributed (i.ni.d.) Nakagami-*m* RVs with corresponding severity parameters $\{m_{ci}\}_{i=1}^M$ and average powers $\{\Omega_{ci}\}_{i=1}^M$.

The overall communication takes place in two temporal phases by employing opportunistic scheduling of users. In the first phase, satellite S beamforms its unit energy signal x_s to the relay R. The received signal at R can be expressed as

$$y_r = \sqrt{P_s}\mathbf{h}_{sr}^\dagger \mathbf{w}_{sr} x_s + \sum_{i=1}^{M} \sqrt{P_{ci}} h_{ir} x_i + n_r, \tag{1}$$

where P_s is the transmit power at S, $\mathbf{w}_{sr}$ is the $N_s \times 1$ transmit weight vector, P_{ci} is the transmit power of the ith interferer, x_i is the unit energy signal of the ith interferer, and $n_r \sim \mathcal{CN}(0, \sigma^2)$ is AWGN at relay R. The transmit beamforming vector $\mathbf{w}_{sr} \in \mathbb{C}^{N_s \times 1}$ is chosen according to the principle of MRT [40] as $\mathbf{w}_{sr} = \frac{\mathbf{h}_{sr}}{||\mathbf{h}_{sr}||_F}$. Note that this requires CSI

[4] This could be possible when the AF relay lies close to other earth stations and/or other relays and/or clusters of non-targeted land users, while it cannot support advanced interference management techniques. As such, the relay in our proposed system model may encounter a CCI environment.

for the satellite-relay links only and hence may offer a low implementation complexity.[5]

During the second phase, the relay R first amplifies the received signal y_r by a gain factor $\mathcal{G}$ and then forwards it to the selected destination D_n. Hence, the received signal at D_n after MRC is expressed as

$$y_{d_n} = \mathcal{G}\sqrt{P_r}\mathbf{w}_{rd_n}^{\dagger}\mathbf{h}_{rd_n}y_r + \mathbf{w}_{rd_n}^{\dagger}\mathbf{n}_{d_n}, \tag{2}$$

where P_r is the transmit power at R, w_{rd_n} is the $N_d \times 1$ receive weight vector, and $\mathbf{n}_{d_n} \sim \mathcal{CN}(\mathbf{0}, \sigma^2 I)$ is the $N_d \times 1$ AWGN vector. According to the MRC principle [40], the receive beamforming vector is chosen as $\mathbf{w}_{rd_n} = \frac{\mathbf{h}_{rd_n}}{||\mathbf{h}_{rd_n}||_F}$. Thus, based on (2), the end-to-end signal-to-interference-plus-noise-ratio (SINR) can be obtained as

$$\gamma_{sd_n} = \frac{\gamma_{sr}\gamma_{rd_n}}{\gamma_{rd_n}(\gamma_c + 1) + \frac{1}{\mathcal{G}^2\sigma^2}}, \tag{3}$$

where $\gamma_{sr} = \eta_s||\mathbf{h}_{sr}||_F^2$, $\gamma_{rd_n} = \eta_r||\mathbf{h}_{rd_n}||_F^2$, $\gamma_c = \sum_{i=1}^{M}\eta_{ci}|h_{ir}|^2$, with $\eta_s = \frac{P_s}{\sigma^2}$, $\eta_r = \frac{P_r}{\sigma^2}$ and $\eta_{ci} = \frac{P_{ci}}{\sigma^2}$. For variable gain relaying, the gain $\mathcal{G}$ in (3) can be determined as

$$\mathcal{G} = \sqrt{\frac{1}{P_s|\mathbf{h}_{sr}^{\dagger}\mathbf{w}_{sr}|^2 + \sum_{i=1}^{M}P_{ci}|h_{ir}|^2 + \sigma^2}}, \tag{4}$$

wherein it is assumed that the amplification process is performed by a simple normalization of the total received power at the relay without applying any interference mitigation technique, as widely adopted in similar studies [10], [14], [28]. Thus, the instantaneous end-to-end SINR at the nth destination is given by

$$\gamma_{sd_n} = \frac{\gamma_{sr}\gamma_{rd_n}}{\gamma_{sr} + (\gamma_{rd_n} + 1)(\gamma_c + 1)}. \tag{5}$$

To harness the multiuser diversity inherent in the considered network, an opportunistic scheduling of D_n is employed, wherein the transmissions are scheduled based on the channel quality of multiple destinations with the relay. For this, the relay first selects the destination with the strongest R-D_n link, and then feeds back the index of the selected user to the satellite S. As such, the instantaneous SNR of the relay-user link is formulated by

$$\gamma_{rd} = \max_{n=1,\ldots,N}\gamma_{rd_n}. \tag{6}$$

In realistic scenarios, where the channel changes rapidly enough, the CSI obtained by the relay could be outdated [41]. Thereby, a delay exists between the user selection phase and the data transmission phase. Hence, the actual end-to-end SINR associated with the scheduled user can be given by

$$\gamma_{sd} = \frac{\gamma_{sr}\widetilde{\gamma}_{rd}}{\gamma_{sr} + (\widetilde{\gamma}_{rd} + 1)(\gamma_c + 1)}, \tag{7}$$

[5]This is in contrast to other beamforming schemes which may require CSI of overall links to attain a better performance. It would however be very difficult for the satellite to acquire the CSI of interfering links as well as that of multi-antenna multiuser links over the second hop in practice.

where $\widetilde{\gamma}_{rd}$ is the delayed version of γ_{rd}. Let $\widetilde{\gamma}_{rd_n}$ be the delayed version of γ_{rd_n} and is given by $\widetilde{\gamma}_{rd_n} = \eta_r||\widetilde{\mathbf{h}}_{rd_n}||_F^2$, where $\widetilde{\mathbf{h}}_{rd_n}$ is the delayed version of $\mathbf{h}_{rd_n}$. The correlation coefficient between $\widetilde{\gamma}_{rd_n}$ and γ_{rd_n} can be given by $\rho_{rd} = J_0^2(2\pi f_o\tau)$ [42] with $J_0(\cdot)$ being the zeroth-order Bessel function of the first kind [49, eq. (8.411)], f_o is the Doppler frequency, and τ is the time delay.

III. PERFORMANCE ANALYSIS WITH UNCORRELATED SHADOWED-RICIAN FADING

In this section, we present OP and EC analysis for the HSTRN as described previously in the presence of uncorrelated Shadowed-Rician fading of $S-R$ link. We also deduce the achievable diversity order of the system by carrying out an asymptotic OP analysis at high SNR.

Herein, we consider the channel vector $\mathbf{h}_{sr}$ with i.i.d. Shadowed-Rician fading entries. As such, the PDF of the squared amplitude of the channel coefficient $h_{sr}^{(\iota)}$ between satellite's ιth antenna and the relay is given by [6], [36]

$$f_{|h_{sr}^{(\iota)}|^2}(x) = \alpha e^{-\beta x}\,{}_1F_1(m_s; 1; \delta x), \quad x \geq 0, \tag{8}$$

where $\alpha = (2bm_s/(2bm_s + \Omega_s))^{m_s}/2b$, $\beta = 1/2b$, and $\delta = \Omega_s/(2b(2bm_s + \Omega_s))$ with Ω_s and $2b$ being the average power of LOS and multipath components, respectively, m_s is the fading severity parameter, and ${}_1F_1(\cdot;\cdot;\cdot)$ is the confluent hypergeometric function of the first kind [49, eq. (9.210.1)].

Throughout this paper, we resort to the integer values of the Shadowed-Rician fading severity parameter [27] for analytical tractability. In fact, the hypergeometric function can be represented via Kummer's transform [43] as

$${}_1F_1(a; b; x) = e^x\sum_{n=0}^{a-b}\frac{(a-b)!x^n}{(a-b-n)!n!(b)_n}, \tag{9}$$

where $(\cdot)_n$ is the Pochhammer symbol [49, p. xliii]. Thereby, for integer m_s, we can simplify ${}_1F_1(m_s; 1; \delta x)$ to represent the PDF in (8) as

$$f_{|h_{sr}^{(\iota)}|^2}(x) = \alpha\sum_{\kappa=0}^{m_s-1}\psi(\kappa)x^{\kappa}e^{-(\beta-\delta)x}, \tag{10}$$

with $\psi(\kappa) = (-1)^{\kappa}(1-m_s)_{\kappa}\delta^{\kappa}/(\kappa!)^2$.

Lemma 1: The PDF and CDF of γ_{sr} under i.i.d. Shadowed-Rician fading can be given, respectively, by

$$f_{\gamma_{sr}}(x) = \sum_{i_1=0}^{m_s-1}\cdots\sum_{i_{N_s}=0}^{m_s-1}\frac{\Xi(N_s)}{\eta_s^{\Lambda}}x^{\Lambda-1}e^{-\beta_{\delta}x} \tag{11}$$

and

$$F_{\gamma_{sr}}(x) = 1 - \sum_{i_1=0}^{m_s-1}\cdots\sum_{i_{N_s}=0}^{m_s-1}\frac{\Xi(N_s)}{\eta_s^{\Lambda}}\sum_{p=0}^{\Lambda-1}\frac{\Gamma(\Lambda)}{p!} \times\beta_{\delta}^{-(\Lambda-p)}x^p e^{-\beta_{\delta}x}, \tag{12}$$

where

$$\Xi(N_s) = \alpha^{N_s} \prod_{\kappa=1}^{N_s} \psi(i_\kappa) \prod_{j=1}^{N_s-1} \mathcal{B}\left(\sum_{l=1}^{j} i_l + j, i_{j+1} + 1\right),$$

$$\beta_\delta = \frac{\beta - \delta}{\eta_s}, \quad \Lambda = \sum_{\kappa=1}^{N_s} i_\kappa + N_s,$$

and $\mathcal{B}(.,.)$ denotes the Beta function [49, eq. (8.384.1)].

Proof: The PDF in (11) can be derived by following the procedure given in [27, Appendix A] and making a transformation of variates. The corresponding CDF in (12) can be obtained by integrating the PDF in (11) with the aid of [49, eq. (3.351.2)]. ∎

Considering the terrestrial links with a cluster of $\{D_n\}_{n=1}^{N}$ users, the pertinent channels follow i.i.d. Nakagami-m fading[6] with fading severity m_d and average power Ω_d. As such, the PDF and CDF of channel gain γ_{rd_n} are given, respectively, by

$$f_{\gamma_{rd_n}}(x) = \left(\frac{m_d}{\Omega_d \eta_r}\right)^{m_d N_d} \frac{x^{m_d N_d - 1}}{\Gamma(m_d N_d)} \mathrm{e}^{-\frac{m_d x}{\Omega_d \eta_r}} \tag{13}$$

and

$$F_{\gamma_{rd_n}}(x) = \frac{1}{\Gamma(m_d N_d)} \Upsilon\left(m_d N_d, \frac{m_d x}{\Omega_d \eta_r}\right). \tag{14}$$

Lemma 2: The PDF of $\widetilde{\gamma}_{rd}$ can be given by

$$f_{\widetilde{\gamma}_{rd}}(x) = N \sum_{j=0}^{N-1} \mathcal{C}_j^{N-1} \frac{(-1)^j}{\Gamma(m_d N_d)} \sum_{l=0}^{j(m_d N_d - 1)} \omega_l^j \sum_{i=0}^{l} \mathcal{C}_i^l \times \left(\frac{m_d}{\Omega_d \eta_r}\right)^{m_d N_d + i} \xi_{i,j,l}\, x^{m_d N_d - 1 + i} \mathrm{e}^{-\frac{x}{\chi_j}}, \tag{15}$$

where $\xi_{i,j,l} = \frac{\Gamma(m_d N_d + l)\rho_{rd}^i (1-\rho_{rd})^{l-i}}{\Gamma(m_d N_d + i)[j(1-\rho_{rd})+1]^{m_d N_d + l + i}}$, $\chi_j = \frac{[j(1-\rho_{rd})+1]\Omega_d \eta_r}{m_d (j+1)}$ and the coefficients ω_l^j, for $0 \le l \le j(m_d N_d - 1)$, can be calculated recursively (with $\varepsilon_l = \frac{1}{l!}$) as $\omega_0^j = (\varepsilon_0)^j$, $\omega_1^j = j(\varepsilon_1)$, $\omega_{j(m_d N_d - 1)}^j = (\varepsilon_{m_d N_d - 1})^j$, $\omega_l^j = \frac{1}{l\varepsilon_0} \sum_{g=1}^{l} [gj - l + g] \varepsilon_g \omega_{l-g}^j$ for $2 \le l \le m_d N_d - 1$, and $\omega_l^j = \frac{1}{l\varepsilon_0} \sum_{g=1}^{m_d N_d - 1} [gj - l + g] \varepsilon_g \omega_{l-g}^j$ for $m_d N_d \le l < j(m_d N_d - 1)$.

Proof: By applying order statistics, the PDF of γ_{rd} can be represented as

$$f_{\gamma_{rd}}(x) = N[F_{\gamma_{rd_n}}(x)]^{N-1} f_{\gamma_{rd_n}}(x), \quad x \ge 0. \tag{16}$$

On invoking the CDF $F_{\gamma_{rd_n}}(x)$ with series form of $\Upsilon(\cdot,\cdot)$ [49, eq. (8.352.1)] and the respective PDF into (16), and then applying binomial and multinomial expansions [49, eq. (0.314)], we get

$$f_{\gamma_{rd}}(x) = N \sum_{j=0}^{N-1} \mathcal{C}_j^{N-1} \frac{(-1)^j}{\Gamma(m_d N_d)} \sum_{l=0}^{j(m_d N_d - 1)} \left(\frac{m_d}{\Omega_d \eta_r}\right)^{m_d N_d + l} \times \omega_l^j x^{m_d N_d + l - 1} \mathrm{e}^{-\frac{m_d (j+1) x}{\Omega_d \eta_r}}. \tag{17}$$

[6] As in various works [14], [28], we follow i.i.d. assumption for terrestrial users to keep the system performance analysis tractable. Such a scenario may however be realized in practice when the terrestrial users are clustered relatively close together (location-based clustering).

Since $\widetilde{\gamma}_{rd}$ and γ_{rd} are correlated Gamma-distributed RVs, the PDF of $\widetilde{\gamma}_{rd}$ can be obtained as

$$f_{\widetilde{\gamma}_{rd}}(x) = \int_0^\infty f_{\widetilde{\gamma}_{rd}|\gamma_{rd}}(x|y) f_{\gamma_{rd}}(y) dy, \tag{18}$$

where $f_{\widetilde{\gamma}_{rd}|\gamma_{rd}}(x|y)$ is the conditional PDF of $\widetilde{\gamma}_{rd}$, conditioned on γ_{rd}. It can be given by [40]

$$f_{\widetilde{\gamma}_{rd}|\gamma_{rd}}(x|y) = \frac{1}{(1-\rho_{rd})} \left(\frac{m_d}{\Omega_d \eta_r}\right) \left(\frac{x}{\rho_{rd} y}\right)^{\frac{m_d N_d - 1}{2}} \times \mathrm{e}^{-\frac{m_d (\rho_{rd} y + x)}{(1-\rho_{rd})\Omega_d \eta_r}} \mathcal{I}_{m_d N_d - 1}\left(\frac{2 m_d \sqrt{\rho_{rd} x y}}{(1-\rho_{rd})\Omega_d \eta_r}\right), \tag{19}$$

where $\mathcal{I}_\nu(\cdot)$ is the νth order modified Bessel function of the first kind [49, eq. (8.406.1)]. On substituting (19) and (17) into (18), and simplifying using the approach in [42], we obtain (15). ∎

Now, differently from $f_{\gamma_{sr}}(x)$ and $f_{\widetilde{\gamma}_{rd}}(x)$, the derivation of exact PDF of γ_c is rather intractable since it involves the sum of i.ni.d. Gamma RVs and hence needs to perform a multifold convolution, becoming cumbersome even for small number of interferers. Therefore, as in [44] and [45], we resort to a highly accurate approximation approach [46] by which the PDF of γ_c can be represented effectively to that of a single Gamma RV as

$$f_{\gamma_c}(x) \approx \left(\frac{m_I}{\Omega_I}\right)^{m_I} \frac{x^{m_I - 1}}{\Gamma(m_I)} \mathrm{e}^{-\frac{m_I}{\Omega_I} x}, \tag{20}$$

where the parameters m_I and Ω_I are calculated from moment-based estimators. For this, we define $\Phi = \sum_{i=1}^{M} |h_{ir}|^2$ and, without loss of generality, we assume no power control is used i.e., $P_{ci} = P_c$ or $\eta_{ci} = \eta_c = \frac{P_c}{\sigma^2}$. Then, from [44] and [45], we have $\Omega_I = \eta_c \Omega_c$ with $\Omega_c = E[\Phi] = \sum_{i=1}^{M} \Omega_{ci}$ and $m_I = \frac{\Omega_c^2}{E[\Phi^2] - \Omega_c^2}$. Herein, the exact moments of Φ can be obtained in terms of the individual moments of the summands as

$$E[\Phi^n] = \sum_{n_1=0}^{n} \sum_{n_2=0}^{n_1} \cdots \sum_{n_{M-1}=0}^{n_{M-2}} \binom{n}{n_1} \binom{n_1}{n_2} \cdots \binom{n_{M-2}}{n_{M-1}} \times E\left[|h_{1r}|^{2(n-n_1)}\right] E\left[|h_{2r}|^{2(n_1-n_2)}\right] \cdots E\left[|h_{Mr}|^{2(n_{M-1})}\right], \tag{21}$$

where

$$E\left[|h_{ir}|^n\right] = \frac{\Gamma\left(m_{ci} + \frac{n}{2}\right)}{\Gamma(m_{ci})} \left(\frac{\Omega_{ci}}{m_{ci}}\right)^{\frac{n}{2}}. \tag{22}$$

A. OUTAGE PROBABILITY

The OP is defined as the probability that the instantaneous end-to-end SINR γ_{sd} falls below a certain threshold γ_{th}. It can be mathematically represented as

$$\mathcal{P}_{\text{out}} = \Pr[\gamma_{sd} < \gamma_{\text{th}}] = F_{\gamma_{sd}}(\gamma_{\text{th}}). \tag{23}$$

In order to evaluate OP in (23), we derive the required CDF of γ_{sd} in the following theorem.

$$F_{\gamma_{sd}}(x) = 1 - N \sum_{i_1=0}^{m_s-1} \cdots \sum_{i_{N_s}=0}^{m_s-1} \frac{\Xi(N_s)}{\eta_s^{\Lambda}} \sum_{p=0}^{\Lambda-1} \frac{\Gamma(\Lambda)}{p!} \sum_{j=0}^{N-1} \mathcal{C}_j^{N-1} \frac{(-1)^j}{\Gamma(m_d N_d)} \sum_{l=0}^{j(m_d N_d-1)} \omega_l^j \sum_{i=0}^{l} \mathcal{C}_i^l$$
$$\times \left(\frac{m_d}{\Omega_d \eta_r}\right)^{m_d N_d+i} \xi_{i,j,I} \mathrm{e}^{-\frac{x}{\chi_j}} \sum_{q=0}^{p} \mathcal{C}_q^p \sum_{\nu=0}^{m_d N_d+i-1} \mathcal{C}_\nu^{m_d N_d+i-1} \beta_\delta^{-\Lambda+p+\frac{\nu-q}{2}} \chi_j^{1+\frac{\nu-q}{2}} (1+x)^{\frac{\nu+q}{2}}$$
$$\times x^{m_d N_d+i+p-1-\left(\frac{\nu+q}{2}\right)} \frac{1}{\Gamma(m_I)} \left(\frac{m_I}{\Omega_I}\right)^{m_I} \Gamma(1+p+m_I+\nu-q)\, \Gamma(p+m_I)\, \vartheta_{x,I}^{-\frac{1}{2}[2(p+m_I)+\nu-q]}$$
$$\times \mathrm{e}^{\frac{\beta_\delta x(1+x)}{2\vartheta_{x,I}\chi_j}} \mathcal{W}_{-\frac{1}{2}[2(p+m_I)+\nu-q],\frac{1}{2}(\nu-q+1)}\left(\frac{\beta_\delta x(1+x)}{\vartheta_{x,I}\chi_j}\right). \quad (24)$$

Theorem 1: The closed-form expression of CDF $F_{\gamma_{sd}}(x)$, under uncorrelated Shadowed-Rician fading, can be given as (24) on top of this page, where $\vartheta_{x,I} = \beta_\delta x + \frac{m_I}{\Omega_I}$ and $\mathcal{W}_{u,v}(\cdot)$ is the Whittaker function [49, eq. (9.222)].

Proof: See Appendix A. ∎

Now, by substituting (24) into (23), the OP for HSTRN can be computed directly at $x = \gamma_{\text{th}}$.

Thus, Theorem 1 presents an analytical expression for the precise OP evaluation of the considered HSTRN, and it allows for the complicated hybrid channel scenario in the presence of outdated CSI and CCI with arbitrary number of antennas, number of interferers, and number of users over entire SNR regime. Although the expression in (24) involves gamma and Whittaker functions, it can be efficiently computed using symbolic software packages such as Matlab and Mathematica, thereby implying its practical usefulness.

B. ACHIEVABLE DIVERSITY ORDER

Although the analytical OP expression using (24) is quite useful and provide several insights from numerical plots, it is too complex to predict diversity order for the proposed HSTRN. Therefore, we need to obtain an equivalent OP expression in asymptotically large SNR regime that helps in identifying the joint impact of outdated CSI, CCI, system configuration and channel fading parameters on the achievable diversity order. For this, in the high SNR regime, we assume $\eta_s, \eta_r \to \infty$ with the ratio $\frac{\eta_s}{\eta_r}$ held constant. Consequently, we derive the asymptotic CDF of γ_{sd} under two scenarios, namely outdated CSI ($\rho_{rd} < 1$) and perfect CSI ($\rho_{rd} = 1$), under the influence of CCI in the following corollary.

Corollary 1: The CDF $F_{\gamma_{sd}}(x)$ can be represented at high SNR as

$$F_{\gamma_{sd}}(x) \simeq \frac{\alpha^{N_s} x^{N_s}}{N_s!(\eta_s)^{N_s}} \left(\frac{\Omega_I}{m_I}\right)^{N_s} \frac{\Gamma(N_s+m_I)}{\Gamma(m_I)} + \begin{cases} \Psi_1(x), & \text{if } \rho_{rd} < 1 \\ \Psi_2(x), & \text{if } \rho_{rd} = 1, \end{cases} \quad (25)$$

where $\Psi_1(x)$ and $\Psi_2(x)$ are given, respectively, as

$$\Psi_1(x) = N \sum_{j=0}^{N-1} \mathcal{C}_j^{N-1} \frac{(-1)^j}{\Gamma(m_d N_d)} \times \frac{\left(\frac{m_d}{\Omega_d}\right)^{m_d N_d} x^{m_d N_d}}{[j(1-\rho_{rd})+1]^{m_d N_d} (\eta_r)^{m_d N_d}} \quad (26)$$

and

$$\Psi_2(x) = \frac{1}{[\Gamma(m_d N_d+1)]^N} \left(\frac{m_d x}{\Omega_d \eta_r}\right)^{m_d N_d N}. \quad (27)$$

Proof: See Appendix B. ∎

Now, plugging (25) into (23) and evaluating at $x = \gamma_{\text{th}}$, an asymptotic OP expression can be obtained. Thereby, one can examine the achievable diversity order for the considered HSTRN under the following cases.

Case-1: For perfect CSI ($\rho_{rd} = 1$) and low level of CCI ($\eta_c \ll \eta_s$), the achievable diversity order (defined by the smallest negative exponent of η_s or η_r) is $\min(N_s, m_d N_d N)$.

Case-2: For outdated CSI ($\rho_{rd} < 1$) and low level of CCI ($\eta_c \ll \eta_s$), the achievable diversity order is $\min(N_s, m_d N_d)$.

Case-3: For a high level of CCI i.e., when η_c increases in the same level as η_s while maintaining the ratio $\frac{\eta_c}{\eta_s}$ a finite constant, the diversity order reduces to zero regardless of the perfect or outdated CSI cases.

Remark 1: The advantage of a multi-antenna satellite is clearly highlighted by the achievable diversity order of the considered HSTRN. Specifically, with a low level of CCI and perfect CSI condition, the system can exploit multiuser diversity when the number of antennas at satellite is sufficiently high, otherwise the system performance is bottlenecked by the satellite-relay link whose fading parameter m_s does not contribute to the diversity order. Hence, the deployment of multiple antennas at the satellite is important to realize the achievable performance gain. In addition, when the CSI is outdated, the advantage of multiuser diversity cannot be realized.

C. ERGODIC CAPACITY

In this section, we determine analytical expression of EC for the considered HSTRN. The EC (in bits/s/Hz) is defined as the statistical expectation of the instantaneous mutual information between the source and destination. For end-to-end SINR γ_{sd}, it is mathematically expressed as

$$\overline{C} = \frac{1}{2} E\left[\log_2(1+\gamma_{sd})\right], \quad (28)$$

where the factor $1/2$ accounts for two-phase transmissions from S to D_n. On inserting the SINR γ_{sd} from (7) into (28),

$$\overline{C}_1 = \frac{1}{2\ln 2}\sum_{i_1=0}^{m_s-1}\cdots\sum_{i_{N_s}=0}^{m_s-1}\frac{\Xi(N_s)}{\eta_s^{\Lambda}}\sum_{p=0}^{\Lambda-1}\frac{\Gamma(\Lambda)}{p!}\beta_{\delta}^{-(\Lambda-p)}\frac{1}{\Gamma(m_I)}\left(\frac{\Omega_I}{m_I}\right)^{p} G_{2,2}^{2,2}\left[\frac{m_I}{\Omega_I\beta_{\delta}}\middle|\begin{matrix}1+p,1\\1+p,p+m_I\end{matrix}\right]. \tag{34}$$

$$\overline{C}_2 = \frac{N}{2\ln 2}\sum_{i_1=0}^{m_s-1}\cdots\sum_{i_{N_s}=0}^{m_s-1}\frac{\Xi(N_s)}{\eta_s^{\Lambda}}\sum_{p=0}^{\Lambda-1}\frac{\Gamma(\Lambda)}{p!}\beta_{\delta}^{-(\Lambda-p)}\frac{1}{\Gamma(m_I)}\left(\frac{\Omega_I}{m_I}\right)^{p}\sum_{j=0}^{N-1}\mathcal{C}_j^{N-1}\frac{(-1)^j}{\Gamma(m_dN_d)}$$
$$\times\sum_{l=0}^{j(m_dN_d-1)}\omega_l^j\sum_{i=0}^{l}\mathcal{C}_i^l\left(\frac{m_d}{\Omega_d\eta_r}\right)^{m_dN_d+i}\xi_{i,j,l}\,\chi_j^{m_dN_d+i}G_{1,[1:1],0,[2:1]}^{1,1,1,2,1}\left[\frac{m_I}{\Omega_I\beta_{\delta}}\middle|\begin{matrix}-p;\,1;\,1-m_dN_d-i\\--;\,m_I+p,\,1+p;\,0\\ \chi_j\end{matrix}\right]. \tag{35}$$

one can readily represent

$$\overline{C} = \frac{1}{2}E\left[\log_2\left(\frac{(1+\gamma_{sc})(1+\widetilde{\gamma}_{rd})}{1+\gamma_{sc}+\widetilde{\gamma}_{rd}}\right)\right], \tag{29}$$

where $\gamma_{sc} = \frac{\gamma_{sr}}{\gamma_c}$ is defined under the dominance of interference over noise. The direct computation of EC in (29) is cumbersome. Alternatively, we adopt the moment generating function (MGF)-based approach, as in [48], to evaluate EC as

$$\overline{C} = \frac{1}{2\ln 2}\int_0^{\infty}\mathrm{e}^{-s}\widehat{\mathcal{M}}_{\gamma_{sc}}(s)ds - \frac{1}{2\ln 2}\int_0^{\infty}\mathrm{e}^{-s}\widehat{\mathcal{M}}_{\gamma_{sc}}(s)\mathcal{M}_{\widetilde{\gamma}_{rd}}(s)ds, \tag{30}$$

where

$$\widehat{\mathcal{M}}_{\gamma_{sc}}(s) = \int_0^{\infty}\mathrm{e}^{-sx}\left[1-F_{\gamma_{sc}}(x)\right]dx \tag{31}$$

and

$$\mathcal{M}_{\widetilde{\gamma}_{rd}}(s) = \int_0^{\infty}\mathrm{e}^{-sx}f_{\widetilde{\gamma}_{rd}}(x)dx. \tag{32}$$

Hereby, $\widehat{\mathcal{M}}_{\gamma_{sc}}(s)$ and $\mathcal{M}_{\widetilde{\gamma}_{rd}}(s)$ respectively denote the complementary MGF transform and the MGF of γ_{sc} and $\widetilde{\gamma}_{rd}$. Based on (30), we now proceed to derive closed-form expression of EC in the following theorem.

Theorem 2: The EC in (30) under uncorrelated Shadowed-Rician fading can be given as

$$\overline{C} = \overline{C}_1 - \overline{C}_2, \tag{33}$$

where $\overline{C}_1$ and $\overline{C}_2$ are respectively given by (34) and (35), shown on top of this page, where $G_{2,2}^{2,2}[\cdot]$ is the Meijer's G-function [49, eq. (8.2.1.1)] and $G_{1,[1:1],0,[2:1]}^{1,1,1,2,1}[\cdot]$ is the generalized Meijer's G-function of two-variables [50].

Proof: See Appendix C. ∎

Note that the Meijer's G-function can be readily evaluated using built-in function in Mathematica, while the generalized Meijer's G-function can be proficiently evaluated using approach as presented in [52, Table II]. As such, the derived expression in Theorem 2 is quite useful for precise EC performance evaluation of the considered HSTRN in the generic scenario with arbitrary number of antennas, users, and co-channel interferers.

IV. PERFORMANCE ANALYSIS WITH CORRELATED SHADOWED-RICIAN FADING

Considering $\mathbf{R}_s$ as $N_s \times N_s$ positive definite matrix with constituent elements as correlation coefficients of the LOS components of the Shadowed-Rician fading links, we can model the channel vector (as $\mathbf{h}_{sr} = \mathbf{R}_s^{\frac{1}{2}}\bar{\mathbf{h}}_{sr} + \tilde{\mathbf{h}}_{sr}$) [23], [36], where $R_s^{\frac{1}{2}}$ is the matrix square root of $\mathbf{R}_s$. As such, the statistics of γ_{sr} can be evaluated via the following lemma.

Lemma 3: The PDF and CDF of γ_{sr} under correlated Shadowed-Rician fading channels can be represented, respectively, as

$$f_{\gamma_{sr}}(x) = \zeta\sum_{k=0}^{\infty}\varrho_k\sum_{\ell=0}^{m_sN_s+k-N_s}\varpi_{k,\ell}x^{N_s+\ell-1}\mathrm{e}^{-\left(\frac{\varphi}{\eta_s}\right)x} \tag{36}$$

and

$$F_{\gamma_{sr}}(x) = 1-\zeta\sum_{k=0}^{\infty}\varrho_k\sum_{\ell=0}^{m_sN_s+k-N_s}\varpi_{k,\ell}\sum_{p=0}^{N_s+\ell-1}\frac{\Gamma(N_s+\ell)}{p!}\times\left(\frac{\varphi}{\eta_s}\right)^{-(N_s+\ell-p)}x^p\mathrm{e}^{-\left(\frac{\varphi}{\eta_s}\right)x}, \tag{37}$$

where

$$\zeta = \prod_{i=1}^{N_s}\left(\frac{\lambda}{\lambda_i}\right)^{m_s},$$
$$\varrho_k = \frac{\epsilon_k}{(2b)^{N_s}}\left(\frac{2b}{2b+\lambda}\right)^{m_sN_s+k},$$
$$\varpi_{k,\ell} = \frac{(-1)^{\ell}(N_s-m_sN_s-k)_{\ell}}{\eta_s^{N_s+\ell}\ell!\Gamma(N_s+\ell)}\left(\frac{\lambda}{2b(2b+\lambda)}\right)^{\ell},$$

$\varphi = \frac{1}{2b} - \frac{\lambda}{2b(2b+\lambda)}$, $\lambda = \min\{\lambda_i, i = 1,\ldots,N_s\}$, λ_i are the eigenvalues of matrix $\widetilde{\mathbf{R}}_s = \left(\frac{\Omega_s}{m_s}\right)\mathbf{R}_s$, $\epsilon_0 = 1$, and

$$\epsilon_{k+1} = \frac{m_s}{k+1}\sum_{\iota=1}^{k+1}\left[\sum_{i=1}^{N_s}\left(1-\frac{\lambda}{\lambda_i}\right)^{\iota}\right]\epsilon_{k+1-\iota}, \quad k=0,1,2,\ldots$$

Proof: See Appendix D. ∎

A. OUTAGE PROBABILITY

Here, we present the analytical OP expression for the considered HSTRN over correlated Shadowed-Rician fading channels by deriving the pertaining CDF of γ_{sd} in the following theorem.

Theorem 3: The expression of CDF $F_{\gamma_{sd}}(x)$, under correlated Shadowed-Rician fading, can be given by (38), shown on the bottom of this page, where $\vartheta'_{x,I} = \frac{\varphi}{\eta_s}x + \frac{m_I}{\Omega_I}$ and other parameters are the same as defined previously.

Proof: See Appendix E. ∎

Thus, invoking (38) in (23) and evaluating at $x = \gamma_{\text{th}}$ yield the desired OP for correlated Shadowed-Rician fading case.

B. ACHIEVABLE DIVERSITY ORDER

To examine the diversity order of HSTRN under correlated Shadowed-Rician fading channels, we obtain corresponding asymptotic OP expression through the following corollary.

Corollary 2: The CDF $F_{\gamma_{sd}}(x)$ with correlated Shadowed-Rician fading can be represented at high SNR as

$$F_{\gamma_{sd}}(x) \simeq \zeta \sum_{k=0}^{\infty} \frac{\epsilon_k x^{N_s}\Gamma(N_s+m_I)}{(2b)^{N_s}(N_s-1)!(\eta_s)^{N_s}} \left(\frac{2b}{2b+\lambda}\right)^{m_sN_s+k} \times \frac{1}{\Gamma(m_I)}\left(\frac{\Omega_I}{m_I}\right)^{N_s} + \begin{cases} \Psi_1(x), & \text{if } \rho_{rd} < 1 \\ \Psi_2(x), & \text{if } \rho_{rd} = 1, \end{cases} \quad (39)$$

where $\Psi_1(x)$ and $\Psi_2(x)$ are same as defined in Corollary 1.

Proof: See Appendix F. ∎

From above corollary, we can deduce that the achievable diversity order of HSTRN under correlated Shadowed-Rician fading is $\min(N_s, m_dN_dN)$ for $\rho_{rd} = 1$ and $\min(N_s, m_dN_d)$ for $\rho_{rd} < 1$. This is same as obtained previously in Section III-B for the case of uncorrelated Shadowed-Rician fading.

Remark 2: The system diversity order of proposed HSTRN is not affected by correlation in satellite antennas as clear from (39). It is important to note that due to a strong LOS and sparse scattering environment, the channel correlation would exist at the transmitting satellite. However, since the diversity order does not get affected, the deployment of multiple antennas at satellite in HSTRN is greatly motivated for futuristic wireless system design.

C. ERGODIC CAPACITY

The EC under correlated Shadowed-Rician fading is presented in the following theorem.

TABLE 1. Values of the parameters estimated for the interfering signals.

M	2	3	4	5	6
m_I	2.9697	5.4340	8.4317	11.9136	15.4
Ω_I	3.5	6	9.2	12.7	16.7

Theorem 4: The EC in (30) under correlated Shadowed-Rician fading can be given as

$$\overline{C} = \overline{C}_{o1} - \overline{C}_{o2}, \quad (40)$$

where $\overline{C}_{o1}$ and $\overline{C}_{o2}$ are respectively given by (41) and (42) on bottom of the next page.

Proof: See Appendix G. ∎

It is worth mentioning that although the derived expression in Theorem 4 contains infinite series and Meijer's G-function, it can be evaluated efficiently through Mathematica by taking the finite number of terms to achieve the required accuracy, as illustrated numerically in Section V. Thereby, it can facilitate the precise EC performance evaluation of the considered HSTRN under the correlated Shadowed-Rician fading channels with arbitrary number of antennas, users, and co-channel interferers.

V. NUMERICAL AND SIMULATION RESULTS

To evaluate the performance of the considered HSTRN and to assess the usefulness of our derived analytical and asymptotic expressions, we perform numerical investigations and validate the theoretical results through Monte-Carlo simulations in this section. We set $\Omega_d = 1$, $\gamma_{\text{th}} = 0$ dB, $\eta_c = 1$ dB (unless stated otherwise), and $\eta_s = \eta_r$ as transmit SNR. The Shadowed-Rician fading parameters for satellite $(S-R)$ link are considered as $(m_s, b, \Omega_s = 1, 0.063, 0.0007)$ under heavy shadowing and $(m_s, b, \Omega_s = 5, 0.251, 0.279)$ in average shadowing scenario [27]. In addition, the parameters of interference channels have been set as $\{m_{ci}\}_{i=1}^{6} = \{1, 2, 2.5, 3, 3.5, 3.5\}$ and $\{\Omega_{ci}\}_{i=1}^{6} = \{1, 2.5, 2.5, 3.2, 3.5, 4\}$. For each set of interfering signals, the parameters calculated for respective analytical curves are depicted in Table 1.

$$F_{\gamma_{sd}}(x) = 1 - \zeta N \sum_{k=0}^{\infty} \varrho_k \sum_{\ell=0}^{m_sN_s+k-N_s} \varpi_{k,\ell} \sum_{p=0}^{N_s+\ell-1} \frac{\Gamma(N_s+\ell)}{p!} \sum_{j=0}^{N-1} \mathcal{C}_j^{N-1} \frac{(-1)^j}{\Gamma(m_dN_d)} \sum_{l=0}^{j(m_dN_d-1)} \omega_l^j \sum_{i=0}^{l} \mathcal{C}_i^l \times \left(\frac{m_d}{\Omega_d\eta_r}\right)^{m_dN_d+i} \xi_{i,j,l}\, \mathrm{e}^{-\frac{x}{\chi_j}} \sum_{q=0}^{p} \mathcal{C}_q^p \sum_{\nu=0}^{m_dN_d+i-1} \mathcal{C}_\nu^{m_dN_d+i-1} \left(\frac{\varphi}{\eta_s}\right)^{-N_s-\ell+p+\frac{\nu-q}{2}} \chi_j^{1+\frac{\nu-q}{2}} \times (1+x)^{\frac{\nu+q}{2}} x^{m_dN_d+i+p-1-\left(\frac{\nu+q}{2}\right)} \frac{1}{\Gamma(m_I)} \left(\frac{m_I}{\Omega_I}\right)^{m_I} \Gamma(1+p+m_I+\nu-q)\,\Gamma(p+m_I) \times (\vartheta'_{x,I})^{-\frac{1}{2}[2(p+m_I)+\nu-q]} \mathrm{e}^{\frac{\varphi x(1+x)}{2\eta_s\vartheta'_{x,I}\chi_j}} \mathcal{W}_{-\frac{1}{2}[2(p+m_I)+\nu-q],\frac{1}{2}(\nu-q+1)}\left(\frac{\varphi x(1+x)}{\eta_s\vartheta'_{x,I}\chi_j}\right). \quad (38)$$

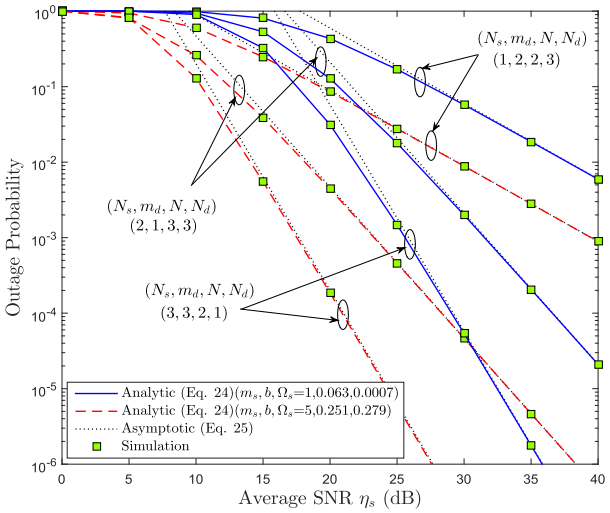

FIGURE 2. OP curves under various diversity parameters.

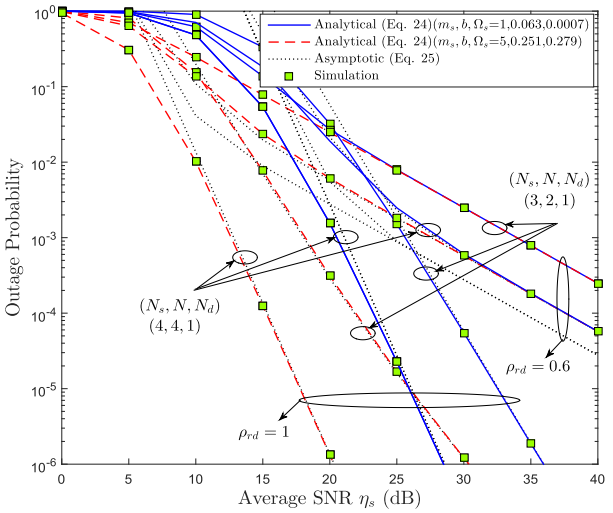

FIGURE 3. Impact of multiple users on OP performance.

A. INVESTIGATION WITH UNCORRELATED SHADOWED-RICIAN FADING

Fig. 2 plots the OP curves versus SNR for the considered HSTRN over uncorrelated Shadowed-Rician faded satellite links and Nakagami-*m* faded terrestrial links. In particular, we obtain the OP curves with various parameters (N_s, m_d, N, N_d) under both average and heavy shadowing scenarios by setting $\rho_{rd} = 0.8$ and number of interferes $M = 3$. The analytical and asymptotic OP curves are plotted using the derived expressions in (24) and (25), respectively, which are clearly found to be aligned and corroborated with the simulation results. From Fig. 2, one can also observe that system's OP curves justify the diversity order of $\min(N_s, m_d N_d)$ as long as the interference power level remains low as compared to transmit power (i.e., $\eta_c \ll \eta_s$). For instance, the diversity order of 3 can be realized through the slopes of the OP curves when (N_s, m_d, N, N_d) being $(3, 3, 2, 1)$ as compared with $(2, 1, 3, 3)$ for diversity order of 2. Accordingly, system's OP performance improves when these diversity parameters increase. Moreover, we can see that the system outage performance becomes better in average fading condition as compared to heavy shadowing scenario, as expected. Indeed, a relative shift in the OP curves can be seen which is due to the system coding gain influenced by system/channel parameters.

Fig. 3 illustrates the impact of multiuser diversity on the system outage performance under both perfect and outdated CSI condition. Herein, we set the fading severity parameter $m_d = 1$ and number of interferers $M = 2$. We can clearly see from this figure that, for a given set of parameters $(N_s, N, N_d) = (3, 2, 1)$, the system exploits multiuser diversity of order 2 in case of perfect CSI ($\rho_{rd} = 1$) while system attains a diversity order of 1 for outdated CSI ($\rho_{rd} = 0.6$) case. The various curves confirm the achievable diversity order of $\min(N_s, m_d N_d N)$ in perfect CSI case and $\min(N_s, m_d N_d)$ in outdated CSI case wherein the multiuser diversity cannot be realized. As such, when $N_s \leq m_d N_d N$, the system performance is dominated by satellite links and hence a notable performance difference appears under heavy and average fading scenarios. Otherwise, if $N_s > m_d N_d N$, the system performance is limited by terrestrial links, and hence the curves for both heavy and average fading scenarios are merging at high SNR e.g., see the respective curves for $(N_s, N, N_d) = (3, 2, 1)$.

Fig. 4 depicts the effect of different interferers and interference power on the outage performance of considered HSTRN. Herein, we plot the OP curves for $M = 1$ and $M = 6$ with a set of interference power $\eta_c = (1, 10)$ dB under both average and heavy Shadowed-Rician fading cases. For this,

$$\overline{C}_{o1} = \frac{\zeta}{2\ln 2}\sum_{k=0}^{\infty}\varrho_k \sum_{\ell=0}^{m_s N_s+k-N_s}\varpi_{k,\ell}\sum_{p=0}^{N_s+\ell-1}\frac{\Gamma(N_s+\ell)}{p!}\left(\frac{\varphi}{\eta_s}\right)^{-(N_s+\ell-p)}\frac{1}{\Gamma(m_I)}\left(\frac{\Omega_I}{m_I}\right)^{p} G_{2,2}^{2,2}\left[\frac{\frac{m_I}{\Omega_I}}{\frac{\varphi}{\eta_s}}\middle|\begin{matrix}1+p, 1\\ 1+p, p+m_I\end{matrix}\right]. \quad (41)$$

$$\overline{C}_{o2} = \frac{\zeta N}{2\ln 2}\sum_{k=0}^{\infty}\varrho_k \sum_{\ell=0}^{m_s N_s+k-N_s}\varpi_{k,\ell}\sum_{p=0}^{N_s+\ell-1}\frac{\Gamma(N_s+\ell)}{p!}\left(\frac{\varphi}{\eta_s}\right)^{-(N_s+\ell-p)}\frac{1}{\Gamma(m_I)}\left(\frac{\Omega_I}{m_I}\right)^{p}\sum_{j=0}^{N-1}\mathcal{C}_j^{N-1}\frac{(-1)^j}{\Gamma(m_d N_d)}$$
$$\times\sum_{l=0}^{j(m_d N_d-1)}\omega_l^j\sum_{i=0}^{l}\mathcal{C}_i^l\left(\frac{m_d}{\Omega_d\eta_r}\right)^{m_d N_d+i}\xi_{i,j,l}\ \chi_j^{m_d N_d+i} G_{1,[1:1],0,[2:1]}^{1,1,1,2,1}\left[\frac{\frac{m_I\eta_s}{\Omega_I\varphi}}{\chi_j}\middle|\begin{matrix}-p;\ 1;\ 1-m_d N_d-i\\ --;\ m_I+p,\ 1+p;\ 0\end{matrix}\right]. \quad (42)$$

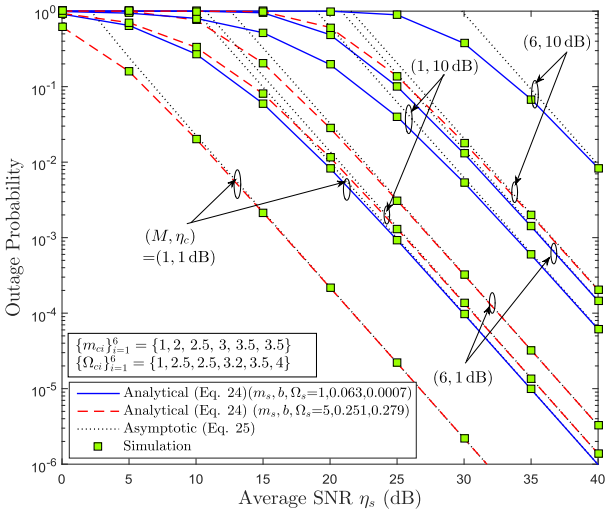

FIGURE 4. Impact of interferers on OP performance.

we set $N_s = 2$, $N = 2$, $m_d = 1$, $N_d = 3$, and $\rho_{rd} = 0.4$. It can be observed from Fig. 4 that, as the number of interferes or interference power increases, the OP performance of the system degrades as revealed clearly by set of curves $(M, \eta_c) = (1, 1\,\text{dB}), (1, 10\,\text{dB}), (6, 1\,\text{dB}), (6, 10\,\text{dB})$. Moreover, the analytical and asymptotic curves corresponding to the OP evaluation for finite number of interferers are found to be very accurate to exact simulation results and they are closely aligned in the high SNR regime.

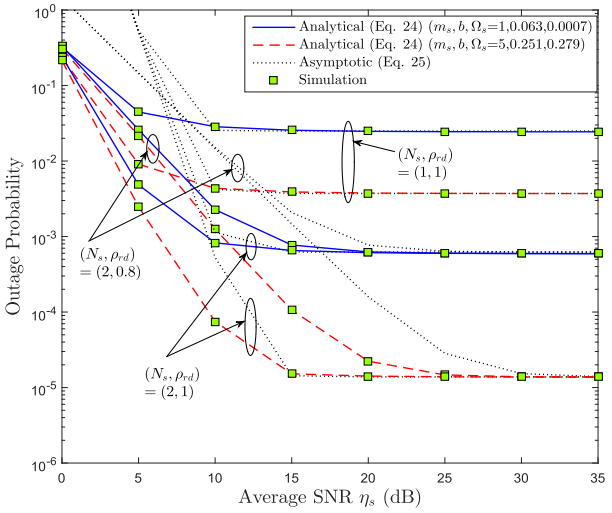

FIGURE 5. Effect of high interference power levels.

Fig. 5 shows the OP curves for the considered HSTRN under high interference power levels, where we set $M = 1$, $N = 3$, $m_d = 2$, and $N_d = 1$. Herein, we consider high interference power η_c such that η_c varies proportionally with η_s, while maintaining $\frac{\eta_s}{\eta_c}$ as a constant ratio of 25 dB. It is observed that the high interference power level brings zero diversity floor to the system performance. Note that for both $\rho_{rd} = 1$ (perfect CSI) and $\rho_{rd} < 1$ (outdated CSI) cases, the system holds zero diversity gain under high interference power level. Further, one can see that the outdated CSI ($\rho_{rd} = 0.8$) degrades the system OP performance. It is worth noting that when CSI is outdated ($\rho_{rd} < 1$) for a fixed number of interferes M, the system OP performance deteriorates owing to the affect on coding gain. Nevertheless, increase in the number of source antennas from $N_s = 1$ to $N_s = 2$ brings improvement in the system outage performance. The agreement between the analytical and asymptotic behaviour is noticeable which is confirmed by simulation, and graphically no visible difference can be found at high SNR.

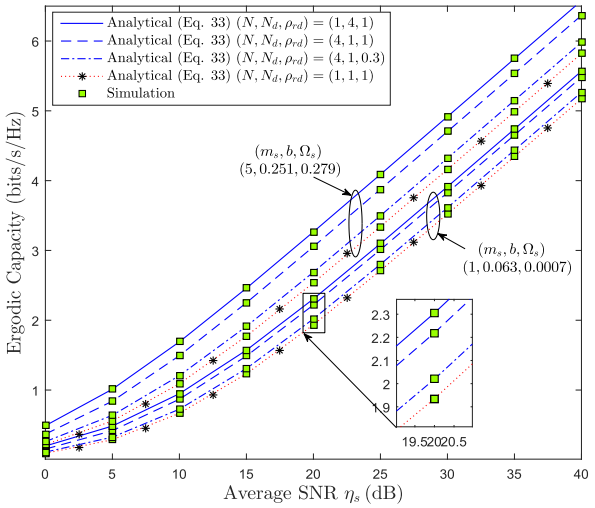

FIGURE 6. Impact of users/destinations with multiple antennas on the system EC performance.

In Fig. 6, curves highlight the impact of number of users/destinations with multiple antennas on the EC performance. Specifically, the EC curves are drawn for the four different sets of parameters (N, N_d, ρ_{rd}) under the setting $N_s = 2$, $m_d = 1$, and $M = 1$. As can be readily observed, the expected result that the EC of the considered system improves when an increase in number of destinations and/or number of antennas at destinations, vindicating the advantages of using multiple destinations with multiple antennas. For example, system configuration with parameters $(N, N_d, \rho_{rd}) = (1, 4, 1)$ and $(4, 1, 1)$ can obtain a capacity enhancement compared with $(1, 1, 1)$. However, it is worth pointing that increasing number of destinations N shows marginal improvement in the system EC under the outdated CSI case (i.e., $\rho_{rd} = 0.3$), whereas significant enhancement can be realized in EC performance by increasing the number of destinations N and/or destination antennas N_d in case of perfect CSI (i.e., $\rho_{rd} = 1$). Hence, as expected system EC performance improves when CSI becomes perfect. Moreover, it is important to observe that system achieves high EC in average fading as compared to heavy fading scenario for the satellite channels. As we can see, for all the cases in this figure, the analytical and corresponding simulation results show perfect agreement.

In Fig. 7, we plot the EC curves for different source antenna configurations under the influence of interferers M and different levels of $\frac{\eta_s}{\eta_c}$ for heavy fading scenarios of satellite

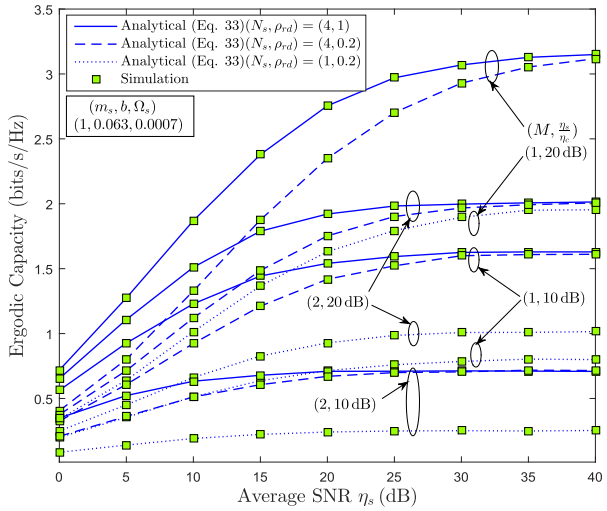

FIGURE 7. Impact of satellite antennas on EC under different interferers and interference levels.

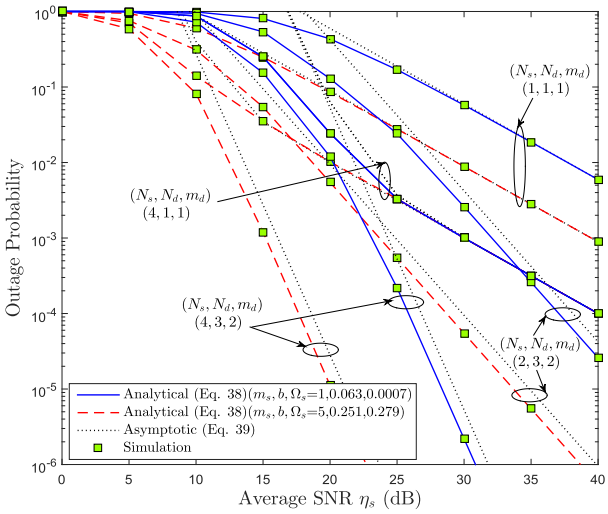

FIGURE 8. OP over correlated Shadowed-Rician fading.

links. For this, we have considered $N = 1$, $N_d = 2$, and $m_d = 2$. It can be clearly observed that EC performance of the considered HSTRN improves with an increase in the number N_s of source antennas. However, diminution in EC is obvious when the number M of interferers or/and interference power level increases. As apparent from the curves, for small number of interferers and low interference power level η_c i.e., $(M, \eta_s/\eta_c) = (1, 20\text{dB})$, the system attains high EC as compared to large number of interferers and high interference power level i.e., $(M, \eta_s/\eta_c) = (2, 10\text{dB})$. Also, one can observe that the system's EC saturates at high SNR owing to the dominating effect of CCI on the system performance. Moreover, it is apparent from the curves that system achieves enhanced EC for perfect CSI ($\rho_{rd} = 1$) over outdated CSI ($\rho_{rd} = 0.2$) case. As seen can be seen from the figure that analytical results perfectly match with the simulation results.

TABLE 2. Number of terms for infinite series calculation.

No. of terms	5	15	25	35	38	40
Eq. (38)	0.5018	0.1671	0.0638	0.0320	0.0257	0.0257
Eq. (39)	0.0215	0.0358	0.0402	0.0415	0.0419	0.0419
Eq. (40)‡	0.83	1.70	2.42	2.63	2.64	2.64

‡in bits/s/Hz.

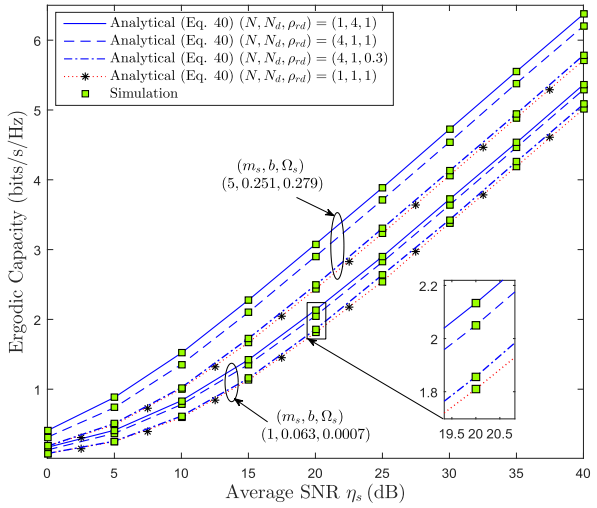

FIGURE 9. EC over correlated Shadowed-Rician fading.

B. INVESTIGATION WITH CORRELATED SHADOWED-RICIAN FADING

In Fig. 8, we study and verify the simulated and analytical OP of HSTRN for the exponentially correlated Shadowed-Rician fading channels of satellite links. Curves are plotted for both average and heavy Shadowed-Rician fading scenarios. Elements of pertaining correlation matrix are generated as $\mathbf{R}_s = [\rho_{i_{p,q}}]$, $p, q = 1, 2, \ldots, N_s$, where correlation coefficient $\rho_{i_{p,q}}$ between the pth and qth antennas of source is given as $\rho_{i_{p,q}} = \rho_i^{|p-q|}$. Herein, the plots are obtained for OP by setting $N = 2, M = 3$, $\rho_{rd} = 0.6$, and $\rho_i = 0.8$. In this figure, all the analytical curves are obtained by truncating the infinite series at 40th term in (38) and (39). We provide Table 2 to reflect the number of terms required for attaining sufficient accuracy.[7] The simulated results corroborate the analytical results. It can be observed further that system attains the same diversity order as obtained in uncorrelated Shadowed-Rician fading case. Thereby, one can clearly see that correlation doesn't affect the system diversity order. Moreover, the performance improvement can be observed when the number of antennas at either source or at destinations increases.

The EC performance is depicted in Fig. 9 over correlated satellite channels for both average and heavy Shadowed-Rician fading scenarios. To obtain the analytical EC curves, we use first 40 terms for infinite series calculation at each SNR value in (40). Herein, the EC curves are drawn for

[7] In Table 2, we have performed computation of (38) and (39) by setting $(N_s, N, M, m_d, N_d, \eta_c, \rho_{rd}, \rho_i) = (2, 2, 3, 2, 3, 1\text{dB}, 0.6, 0.8)$ and of (40) by setting $(N_s, N, M, m_d, N_d, \eta_c, \rho_{rd}, \rho_i) = (2, 4, 1, 1, 1, 1\text{dB}, 0.3, 0.5)$ with the aid of Table 1 at 25 dB SNR under heavy Shadowed-Rician fading.

different sets of parameters as adopted for Fig. 6 and by fixing correlation coefficient $\rho_i = 0.5$. Good agreement between simulated and analytical curves is evident. On comparing the curves in Fig. 6 and Fig. 9, one can infer that owing to correlated fading, the EC of the proposed HSTRN deteriorates. For instance, with a given set of parameters $(N, N_d, \rho_{rd}) = (1, 4, 1)$ under heavy shadowing at 40 dB SNR, one can see that the EC of the system over correlated fading channels is 5.36 bits/s/Hz as illustrated in Fig. 9, whereas EC achieved by system for uncorrelated fading case is 5.56 bits/s/Hz as clear from Fig. 6.

VI. CONCLUSION

We conducted a comprehensive performance analysis of a multiuser AF-based HSTRN by deploying multiple antennas at satellite and users under Shadowed-Rician fading for satellite links and Nakagami-m fading for terrestrial links. Herein, for complexity-aware HSTRN design in real operating conditions, we considered opportunistic scheduling of users with outdated CSI and AF relaying in the presence of CCI signals. We derived accurate and generalized expressions for OP and EC measures of the considered HSTRN by taking into account both uncorrelated and correlated Shadowed-Rician fading channels for satellite links. By further deriving the asymptotic OP expressions, we deduced the achievable diversity orders. We substantiated that the system diversity order is greatly influenced by number of antennas, users and level of CSI and CCI, but independent of the correlation and fading parameter of the LOS in multi-antenna satellite links. Our results identified various key system/channel parameters and provided useful insights for deployment of HSTRN in futuristic wireless systems. A straightforward extension of our present model would lie in the consideration of multiple antennas at the relay to address a more general scenario in practice.

APPENDIX A

The CDF $F_{\gamma_{sd}}(x)$ can be written using (7) as

$$F_{\gamma_{sd}}(x) = \Pr[\gamma_{sd} < x] = \Pr\left[\frac{\gamma_{sr}\widetilde{\gamma}_{rd}}{\gamma_{sr} + (\widetilde{\gamma}_{rd} + 1)(\gamma_c + 1)} < x\right]. \quad (43)$$

Under the interference limited scenario [39], the CDF $F_{\gamma_{sd}}(x)$ in (43) can be simplified and expressed in terms of expectation over γ_c as

$$F_{\gamma_{sd}}(x) = E_{\gamma_c}\left[\int_0^x f_{\widetilde{\gamma}_{rd}}(z)dz + \int_x^\infty F_{\gamma_{sr}}\left(\frac{x(z+1)\gamma_c}{z-x}\right) f_{\widetilde{\gamma}_{rd}}(z)dz\right], \quad (44)$$

which can be simplified further and given as

$$F_{\gamma_{sd}}(x) = 1 - E_{\gamma_c}[\Phi(x, \gamma_c)], \quad (45)$$

where $\Phi(x, \gamma_c)$ is defined by an integral as

$$\Phi(x, \gamma_c) = \int_x^\infty \left[1 - F_{\gamma_{sr}}\left(\frac{x(z+1)\gamma_c}{z-x}\right)\right] f_{\widetilde{\gamma}_{rd}}(z)dz. \quad (46)$$

On invoking the CDF of γ_{sr} from (12) and the PDF of $\widetilde{\gamma}_{rd}$ from (15) into (46), and simplifying subsequently with the help of [49, eqs. (1.111) and (3.471.9)], we obtain the result as given in (47), shown at the top of the next page where $\mathcal{K}_v(\cdot)$ is the modified Bessel function of the second kind and order v [49, eq. (8.432.6)].

Now, by performing the expectation of (47) over γ_c using the PDF from (20) as

$$E_{\gamma_c}[\Phi(x, \gamma_c)] = \int_0^\infty \Phi(x, \gamma_c)|_{\gamma_c = y} f_{\gamma_c}(y)dy, \quad (48)$$

with the aid of [49, eq. (6.641.3)], and finally, by substituting the obtained result in (45), one can reach (24).

APPENDIX B

In the high SNR regime, the end-to-end SINR in (7) can be represented as $\gamma_{sd} \simeq \min\left(\frac{\gamma_{sr}}{\gamma_c}, \widetilde{\gamma}_{rd}\right)$, and hence the CDF $F_{\gamma_{sd}}(x)$ is written as

$$F_{\gamma_{sd}}(x) \simeq \Pr\left[\min\left(\frac{\gamma_{sr}}{\gamma_c}, \widetilde{\gamma}_{rd}\right) < x\right]. \quad (49)$$

By defining the ratio $\gamma_{sc} = \frac{\gamma_{sr}}{\gamma_c}$ and exploiting the independence among the involved RVs in (49), we can express $F_{\gamma_{sd}}(x)$ as

$$F_{\gamma_{sd}}(x) \simeq 1 - \left[1 - F_{\gamma_{sc}}(x)\right]\left[1 - F_{\widetilde{\gamma}_{rd}}(x)\right]. \quad (50)$$

To proceed further, we need to evaluate the asymptotic behavior for the CDFs $F_{\gamma_{sc}}(x)$ and $F_{\widetilde{\gamma}_{rd}}(x)$.

First, for $\eta_s \to \infty$, we can apply the Maclaurin series expansion of the exponential function in (11) to approximate the PDF of γ_{sr} as

$$f_{\gamma_{sr}}(x) \simeq \frac{\alpha^{N_s}}{(N_s - 1)!\eta_s^{N_s}} x^{N_s - 1}, \quad (51)$$

and the corresponding CDF follows asymptotic behavior as

$$F_{\gamma_{sr}}(x) \simeq \frac{\alpha^{N_s}}{(N_s)!\eta_s^{N_s}} x^{N_s}. \quad (52)$$

Then, using (52) and PDF from (20), one can calculate the asymptotic behavior of $F_{\gamma_{sc}}(x)$ as

$$F_{\gamma_{sc}}(x) = \int_0^\infty F_{\gamma_{sr}}(x\,y) f_{\gamma_c}(y)dy \quad (53)$$

$$\simeq \frac{\alpha^{N_s} x^{N_s}}{N_s!(\eta_s)^{N_s}} \left(\frac{\Omega_I}{m_I}\right)^{N_s} \frac{\Gamma(N_s + m_I)}{\Gamma(m_I)}. \quad (54)$$

And, to obtain asymptotic behavior of $F_{\widetilde{\gamma}_{rd}}(\gamma_{\text{th}})$, we first simplify the PDF in (15) for $\eta_r \to \infty$ and then integrate the result. Thereby, the asymptotic behavior of the corresponding CDF can be deduced for $\rho_{rd} < 1$ as

$$F_{\widetilde{\gamma}_{rd}}(x) \simeq N \sum_{j=0}^{N-1} \mathcal{C}_j^{N-1} \frac{(-1)^j}{\Gamma(m_d N_d)} \times \frac{\left(\frac{m_d}{\Omega_d}\right)^{m_d N_d} x^{m_d N_d}}{[j(1 - \rho_{rd}) + 1]^{m_d N_d} (\eta_r)^{m_d N_d}}. \quad (55)$$

$$\Phi(x,\gamma_c)=2N\sum_{i_1=0}^{m_s-1}\cdots\sum_{i_{N_s}=0}^{m_s-1}\frac{\Xi(N_s)}{\eta_s^{\Lambda}}\sum_{p=0}^{\Lambda-1}\frac{\Gamma(\Lambda)}{p!}\sum_{j=0}^{N-1}\mathcal{C}_j^{N-1}\frac{(-1)^j}{\Gamma(m_dN_d)}\sum_{l=0}^{j(m_dN_d-1)}\omega_l^j\sum_{i=0}^{l}\mathcal{C}_i^l$$
$$\times\left(\frac{m_d}{\Omega_d\eta_r}\right)^{m_dN_d+i}\xi_{i,j,l}\mathrm{e}^{-\frac{x}{\chi_j}}\sum_{q=0}^{p}\mathcal{C}_q^p\sum_{v=0}^{m_dN_d+i-1}\mathcal{C}_v^{m_dN_d+i-1}\beta_\delta^{-\Lambda+p+\frac{v-q+1}{2}}\chi_j^{\frac{v-q+1}{2}}(1+x)^{\frac{v+q+1}{2}}$$
$$\times x^{m_dN_d+i+p-\left(\frac{v+q+1}{2}\right)}\gamma_c^{p+\frac{v-q+1}{2}}\mathrm{e}^{-\beta_\delta x\gamma_c}\,\mathcal{K}_{v-q+1}\left(2\sqrt{\frac{\beta_\delta x(1+x)\gamma_c}{\chi_j}}\right). \tag{47}$$

For $\rho_{rd}=1$, the asymptotic behavior of $F_{\widetilde{\gamma}_{rd}}(\gamma_{\mathrm{th}})$ can be obtained straightforwardly as

$$F_{\widetilde{\gamma}_{rd}}(x)\simeq\frac{1}{[\Gamma(m_dN_d+1)]^N}\left(\frac{m_dx}{\Omega_d\eta_r}\right)^{m_dN_dN}. \tag{56}$$

Now, after inserting (54)-(56) in (50), one can obtain (25).

APPENDIX C

Under the hypotheses of Theorem 2, $\overline{C}_1$ can be written as

$$\overline{C}_1=\frac{1}{2\ln 2}\int_0^\infty \mathrm{e}^{-s}\widehat{\mathcal{M}}_{\gamma_{sc}}(s)ds. \tag{57}$$

To evaluate complementary MGF transform of γ_{sc} in (57), first we require the CDF of γ_{sc}. On invoking the CDF from (12) and the PDF from (20) into (53), and after performing the required integration, the CDF $F_{\gamma_{sc}}(x)$ can be derived as

$$F_{\gamma_{sc}}(x)=1-\sum_{i_1=0}^{m_s-1}\cdots\sum_{i_{N_s}=0}^{m_s-1}\frac{\Xi(N_s)}{\eta_s^{\Lambda}}\sum_{p=0}^{\Lambda-1}\frac{\Gamma(\Lambda)}{p!}\beta_\delta^{-(\Lambda-p)}$$
$$\times\frac{\Gamma(p+m_I)}{\Gamma(m_I)}\left(\frac{m_I}{\Omega_I}\right)^{m_I}x^p\left(\beta_\delta x+\frac{m_I}{\Omega_I}\right)^{-(p+m_I)}. \tag{58}$$

Then, on inserting the expression from (58) into (31), we have

$$\widehat{\mathcal{M}}_{\gamma_{sc}}(s)=\int_0^\infty \mathrm{e}^{-sx}\left[\sum_{i_1=0}^{m_s-1}\cdots\sum_{i_{N_s}=0}^{m_s-1}\frac{\Xi(N_s)}{\eta_s^{\Lambda}}\sum_{p=0}^{\Lambda-1}\frac{\Gamma(\Lambda)}{p!}\right.$$
$$\times\beta_\delta^{-(\Lambda-p)}\frac{\Gamma(p+m_I)}{\Gamma(m_I)}\left(\frac{m_I}{\Omega_I}\right)^{m_I}$$
$$\left.\times x^p\left(\beta_\delta x+\frac{m_I}{\Omega_I}\right)^{-(p+m_I)}\right]dx. \tag{59}$$

To compute the integral in (59), we make use of the identities of Meijer's G-function as [51, eqs. (10) and (11)]

$$(1+ax)^{-\ell}=\frac{1}{\Gamma(\ell)}G_{1,1}^{1,1}\left[ax\middle|\begin{matrix}1-\ell\\0\end{matrix}\right]$$
$$\text{and}\quad \mathrm{e}^{-bx}=G_{0,1}^{1,0}\left[bx\middle|\begin{matrix}-\\0\end{matrix}\right]. \tag{60}$$

Thereby, solving the integral in (59) using (60) and [51, eq. (21)], and after simplifying with [49, eq. (9.31.2)], we get

$$\widehat{\mathcal{M}}_{\gamma_{sc}}(s)=\sum_{i_1=0}^{m_s-1}\cdots\sum_{i_{N_s}=0}^{m_s-1}\frac{\Xi(N_s)}{\eta_s^{\Lambda}}\sum_{p=0}^{\Lambda-1}\frac{\Gamma(\Lambda)}{p!}\beta_\delta^{-(\Lambda-p)}\frac{1}{\Gamma(m_I)}$$
$$\times\left(\frac{m_I}{\Omega_I}\right)^{-p}s^{-(p+1)}G_{1,2}^{2,1}\left[\frac{\frac{m_I}{\Omega_I}s}{\beta_\delta}\middle|\begin{matrix}1\\1+p,p+m_I\end{matrix}\right]. \tag{61}$$

On inserting the above result in (57), and then solving the involved integral using [49, eq. (7.813.1)], we get the expression of $\overline{C}_1$ as given in (34).

Further, to evaluate $\overline{C}$ in (30), we need to solve the component $\overline{C}_2$ which can be written as

$$\overline{C}_2=\frac{1}{2\ln 2}\int_0^\infty \mathrm{e}^{-s}\widehat{\mathcal{M}}_{\gamma_{sc}}(s)\mathcal{M}_{\widetilde{\gamma}_{rd}}(s)ds. \tag{62}$$

We proceed by first evaluating the MGF of $\widetilde{\gamma}_{rd}$ from (32) using the PDF from (15) as

$$\mathcal{M}_{\widetilde{\gamma}_{rd}}(s)=N\sum_{j=0}^{N-1}\mathcal{C}_j^{N-1}\frac{(-1)^j}{\Gamma(m_dN_d)}\sum_{l=0}^{j(m_dN_d-1)}\omega_l^j\sum_{i=0}^{l}\mathcal{C}_i^l$$
$$\times\frac{\xi_{i,j,l}\,\chi_j^{m_dN_d+i}}{\left(\frac{m_d}{\Omega_d\eta_r}\right)^{-(m_dN_d+i)}}G_{1,1}^{1,1}\left[\chi_j s\middle|\begin{matrix}1-m_dN_d-i\\0\end{matrix}\right]. \tag{63}$$

Finally, by substituting the results from (61) and (63) in (62), and performing the integration with the aid of [47, eq. (2.6.2)], the expression as given in (35) can be obtained.

APPENDIX D

By following the procedure as given in [43, Th. 2], we can express the PDF of $\gamma\triangleq||\mathbf{h}_{sr}||_F^2$ under correlated Shadowed-Rician fading by

$$f_\gamma(x)=\prod_{i=1}^{N_s}\left(\frac{\lambda}{\lambda_i}\right)^{m_s}\sum_{k=0}^{\infty}\frac{\epsilon_k x^{N_s-1}\mathrm{e}^{-\frac{x}{2b}}}{(2b)^{N_s}\Gamma(N_s)}\left(\frac{2b}{2b+\lambda}\right)^{m_sN_s+k}$$
$$\times{}_1F_1\left(m_sN_s+k;N_s;\frac{x\lambda}{2b(2b+\lambda)}\right), \tag{64}$$

$$\Phi(x,\gamma_c) = N\zeta \sum_{k=0}^{\infty} \varrho_k \sum_{\ell=0}^{m_s N_s+k-N_s} \varpi_{k,\ell} \sum_{p=0}^{N_s+\ell-1} \frac{\Gamma(N_s+\ell)}{p!} \left(\frac{\varphi}{\eta_s}\right)^{-(N_s+\ell-p)} \sum_{j=0}^{N-1} \mathcal{C}_j^{N-1} \frac{(-1)^j}{\Gamma(m_d N_d)} \sum_{l=0}^{j(m_d N_d-1)} \omega_l^j \sum_{i=0}^{l} \mathcal{C}_i^l$$
$$\times \left(\frac{m_d}{\Omega_d \eta_r}\right)^{m_d N_d+i} \xi_{i,j,l}\, x^p \gamma_c^p \sum_{q=0}^{p} \mathcal{C}_q^p (1+x)^q \mathrm{e}^{-\left(\frac{\varphi}{\eta_s}\right)x\gamma_c} \sum_{\nu=0}^{m_d N_d-1+i} \mathcal{C}_\nu^{m_d N_d-1+i} x^{m_d N_d-1+i-\nu} \mathrm{e}^{-\frac{x}{\chi_j}}$$
$$\times 2\left(\frac{\varphi}{\eta_s}(1+x)x\gamma_c\chi_j\right)^{\frac{\nu-q+1}{2}} \mathcal{K}_{\nu-q+1}\left(2\sqrt{\frac{\varphi}{\eta_s\chi_j}(1+x)x\gamma_c}\right). \quad (66)$$

where the involved parameters are defined after (37). For integer m_s, the hypergeometric function in (64) can be represented via Kummer's transform as in (9). Thus, by employing (9) and a transformation of variates, we can obtain the PDF of $\gamma_{sr} = \eta_s\gamma$ as

$$f_{\gamma_{sr}}(x) = \prod_{i=1}^{N_s}\left(\frac{\lambda}{\lambda_i}\right)^{m_s} \sum_{k=0}^{\infty} \frac{\epsilon_k}{(2b)^{N_s}} \left(\frac{2b}{2b+\lambda}\right)^{m_s N_s+k}$$
$$\times \sum_{\ell=0}^{m_s N_s+k-N_s} \frac{(m_s N_s+k-N_s)! x^{N_s+\ell-1}}{(m_s N_s+k-N_s-\ell)!\ell!\Gamma(N_s)(N_s)_\ell}$$
$$\times \frac{1}{\eta_s^{N_s+\ell}} \left(\frac{\lambda}{2b(2b+\lambda)}\right)^{\ell} \mathrm{e}^{-\left(\frac{1}{2b}-\frac{\lambda}{2b(2b+\lambda)}\right)\frac{x}{\eta_s}}. \quad (65)$$

After some straightforward manipulations, the above PDF $f_{\gamma_{sr}}(x)$ can be expressed in a more compact-form as given in (36). Finally, by integrating (36) with the help of [49, eq. (3.351.2)], one can get the corresponding CDF $F_{\gamma_{sr}}(x)$ as presented in (37).

APPENDIX E

To evaluate the CDF $F_{\gamma_{sd}}(x)$ under correlated Shadowed-Rician fading case, we follow the same procedure as in Appendix A. On invoking the CDF from (37) in (46) along with PDF $f_{\widetilde{\gamma}_{rd}}(x)$ from (15), we get $\Phi(x,\gamma_c)$ for correlated Shadowed-Rician fading case, which is given in (66), as shown at the top of this page.

In the sequence, we calculate $E_{\gamma_c}[\Phi(x,\gamma_c)]$ by performing the expectation of (66) using the PDF from (20) along with the fact [49, eq. (6.641.3)]. On substituting the so obtained result in (45), the closed-form CDF $F_{\gamma_{sd}}(x)$ in (38) is achieved.

APPENDIX F

With regard to the correlated case of Corollary 2, the asymptotic expression of $F_{\gamma_{sd}}(x)$ can be evaluated similarly as in Appendix B. To proceed, we need to evaluate the asymptotic behavior for the CDF $F_{\gamma_{sc}}(x)$ over correlated Shadowed-Rician fading channels. For this, we simplify the PDF in (36) for $\eta_s \to \infty$ as

$$f_{\gamma_{sr}}(x) \simeq \zeta \sum_{k=0}^{\infty} \varrho_k \frac{x^{N_s-1}}{(N_s-1)!\eta_s^{N_s}} \mathrm{e}^{-\left(\frac{\varphi}{\eta_s}\right)x}, \quad (67)$$

and the corresponding CDF follows asymptotic behavior as

$$F_{\gamma_{sr}}(x) \simeq \zeta \sum_{k=0}^{\infty} \varrho_k \frac{x^{N_s}}{(N_s-1)!\eta_s^{N_s}}. \quad (68)$$

Then, using (68) and PDF from (20), one can calculate the asymptotic behavior of $F_{\gamma_{sc}}(x)$ in (53) for correlated fading case as

$$F_{\gamma_{sc}}(x) \simeq \zeta \sum_{k=0}^{\infty} \frac{\epsilon_k x^{N_s}}{(2b)^{N_s}(N_s-1)!\eta_s^{N_s}} \left(\frac{2b}{2b+\lambda}\right)^{m_s N_s+k}$$
$$\times \frac{\Gamma(N_s+m_I)}{\Gamma(m_I)} \left(\frac{\Omega_I}{m_I}\right)^{N_s}. \quad (69)$$

And, for $\eta_r \to \infty$, we use asymptotic behavior of $F_{\widetilde{\gamma}_{rd}}(\gamma_{\mathrm{th}})$ as provided in (55) and (56). Finally, after plugging (69), (55), and (56) into (50), we obtain the result in (39).

APPENDIX G

EC for the correlated Shadowed-Rician fading case can be evaluated by using the similar steps as in Appendix C. Under the hypotheses of Theorem 4, $\overline{C}_{o1}$ and $\overline{C}_{o2}$ represent the first and second integral terms in (30), which are equivalent to $\overline{C}_1$ in (57) and $\overline{C}_2$ in (62), respectively. Thereby, to evaluate $\overline{C}_{o1}$, we require the complementary MGF transform of γ_{sc}, which can be calculated by invoking CDF $F_{\gamma_{sc}}(x)$ in (31) for correlated fading case. For this, we first obtain the CDF of γ_{sc}, by using (37) and (20) in (53), as

$$F_{\gamma_{sc}}(x) = 1 - \zeta \sum_{k=0}^{\infty} \varrho_k \sum_{\ell=0}^{m_s N_s+k-N_s} \varpi_{k,\ell} \sum_{p}^{N_s+\ell-1} \frac{\Gamma(N_s+\ell)}{p!}$$
$$\times \left(\frac{\varphi}{\eta_s}\right)^{-(N_s+\ell-p)} \frac{\Gamma(p+m_I)}{\Gamma(m_I)} \left(\frac{m_I}{\Omega_I}\right)^{m_I}$$
$$\times x^p \left(\frac{\varphi}{\eta_s}x + \frac{m_I}{\Omega_I}\right)^{-(p+m_I)}. \quad (70)$$

Now, substituting (70) in (31) and solving involved integral with the aid of (60), [51, eq. (21)], and [49, eq. (9.31.2)], $\widehat{\mathcal{M}}_{\gamma_{sc}}(s)$ can be obtained as

$$\widehat{\mathcal{M}}_{\gamma_{sc}}(s) = \zeta \sum_{k=0}^{\infty} \varrho_k \sum_{\ell=0}^{m_s N_s+k-N_s} \varpi_{k,\ell} \sum_{p}^{N_s+\ell-1} \frac{\Gamma(N_s+\ell)}{p!}$$
$$\times \left(\frac{\varphi}{\eta_s}\right)^{-(N_s+\ell-p)} \frac{1}{\Gamma(m_I)} \left(\frac{\Omega_I}{m_I}\right)^{p}$$
$$\times s^{-(p+1)} G_{1,2}^{2,1}\left[\frac{\frac{m_I}{\Omega_I}s}{\frac{\varphi}{\eta_s}}\middle| \begin{matrix} 1 \\ 1+p, p+m_I \end{matrix}\right]. \quad (71)$$

Then, invoking (71) in (57), $\overline{C}_{o1}$ can be solved and thus given as in (41). And in the similar way, plugging (71) and (63) in (62), one can get $\overline{C}_{o2}$ as given in (42).

ACKNOWLEDGMENT

This publication is an outcome of the R&D work undertaken in the project under the Visvesvaraya Ph.D. Scheme of Ministry of Electronics and Information Technology (MeitY), Government of India, being implemented by Digital India Corporation (formerly Media Lab Asia).

REFERENCES

[1] *Digital Video Broadcasting (DVB); System Specifications for Satellite Services to Handheld Devices (SH) Below 3 GHz*, document ETSI EN 102 585 V1.1.2, Apr. 2008.

[2] B. Evans *et al.*, "Integration of satellite and terrestrial systems in future multimedia communications," *IEEE Trans. Wireless Commun.*, vol. 12, no. 5, pp. 72–80, Oct. 2005.

[3] B. Paillassa, B. Escrig, R. Dhaou, M.-L. Boucheret, and C. Bes, "Improving satellite services with cooperative communications," *Int. J. Satellite Commun.*, vol. 29, no. 6, pp. 479–500, 2011.

[4] V. K. Sakarellos, C. Kourogiorgas, and A. K. Panagopoulos, "Cooperative hybrid land mobile satellite–terrestrial broadcasting systems: Outage probability evaluation and accurate simulation," *Wireless Pers. Commun.*, vol. 79, no. 2, pp. 1471–1481, Nov. 2014.

[5] P. Chini, G. Giambene, and S. Kota, "A survey on mobile satellite systems," *Int. J. Satellite Commun.*, vol. 28, no. 1, pp. 29–57, 2010.

[6] M. R. Bhatnagar and M. K. Arti, "Performance analysis of AF based hybrid satellite-terrestrial cooperative network over generalized fading channels," *IEEE Commun. Lett.*, vol. 17, no. 10, pp. 1912–1915, Oct. 2013.

[7] M. R. Bhatnagar and M. K. Arti, "Performance analysis of hybrid satellite-terrestrial FSO cooperative system," *IEEE Photon. Technol. Lett.*, vol. 25, no. 22, pp. 2197–2200, Nov. 15, 2013.

[8] U. Javed, D. He, and P. Liu, "Performance characterization of a hybrid satellite-terrestrial system with co-channel interference over generalized fading channels," *Sensors*, vol. 16, no. 8, p. 1236, 2016.

[9] M. Lin, J. Ouyang, and W.-P. Zhu, "On the performance of hybrid satellite-terrestrial cooperative networks with interferences," in *Proc. 48th Asilomar Conf. Signals, Syst. Comput. (ACSSC)*, Pacific Grove, CA, USA, Nov. 2014, pp. 1796–1800.

[10] L. Yang and M. O. Hasna, "Performance analysis of amplify-and-forward hybrid satellite-terrestrial networks with cochannel interference," *IEEE Trans. Commun.*, vol. 63, no. 12, pp. 5052–5061, Dec. 2015.

[11] S. Sreng, B. Escrig, and M.-L. Boucheret, "Exact symbol error probability of hybrid/integrated satellite-terrestrial cooperative network," *IEEE Trans. Wireless Commun.*, vol. 12, no. 3, pp. 1310–1319, Mar. 2013.

[12] K. An, J. Ouyang, M. Lin, and T. Liang, "Outage analysis of multi-antenna cognitive hybrid satellite-terrestrial relay networks with beamforming," *IEEE Commun. Lett.*, vol. 19, no. 7, pp. 1157–1160, Jul. 2015.

[13] K. An *et al.* "Symbol error analysis of hybrid satellite-terrestrial cooperative networks with co-channel interference," *IEEE Commun. Lett.*, vol. 18, no. 11, pp. 1947–1950, Nov. 2014.

[14] K. T. Hemachandra and N. C. Beaulieu, "Outage analysis of opportunistic scheduling in dual-hop multiuser relay networks in the presence of interference," *IEEE Trans. Commun.*, vol. 61, no. 5, pp. 1786–1796, May 2013.

[15] L. Erwu, W. Dongyao, L. Jimin, S. Gang, and J. Shan, "Performance evaluation of bandwidth allocation in 802.16j mobile multi-hop relay networks," in *Proc. IEEE VTC-Spring*, Dublin, Ireland, Apr. 2007, pp. 939–943.

[16] K. An, M. Lin, and T. Liang, "On the performance of multiuser hybrid satellite-terrestrial relay networks with opportunistic scheduling," *IEEE Commun. Lett.*, vol. 19, no. 10, pp. 1722–1725, Oct. 2015.

[17] P. K. Upadhyay and P. K. Sharma, "Max-max user-relay selection scheme in multiuser and multirelay hybrid satellite-terrestrial relay systems," *IEEE Commun. Lett.*, vol. 20, no. 2, pp. 268–271, Feb. 2016.

[18] P. K. Upadhyay and P. K. Sharma, "Multiuser hybrid satellite-terrestrial relay networks with co-channel interference and feedback latency," in *Proc. Eur. Conf. Netw. Commun. (EuCNC)*, Athens, Greece, Jun. 2016, pp. 174–178.

[19] P. Arapoglou, K. Liolis, M. Bertinelli, A. Panagopoulos, P. Cottis, and R. De Gaudenzi, "MIMO over satellite: A review," *IEEE Commun. Surv. Tuts.*, vol. 13, no. 1, pp. 27–51, 1st Quart., 2011.

[20] K. P. Liolis, A. D. Panagopoulos, and P. G. Cottis, "Multi-satellite MIMO communications at Ku-band and above: Investigations on spatial multiplexing for capacity improvement and selection diversity for interference mitigation," *EURASIP J. Wireless Commun. Netw.*, vol. 2007, no. 2, p. 16, Jan. 2007.

[21] P. Petropoulou, E. T. Michailidis, A. D. Panagopoulos, and A. G. Kanatas, "Radio propagation channel measurements for multi-antenna satellite communication systems: A survey," *IEEE Antennas Propag. Mag.*, vol. 56, no. 6, pp. 102–122, Dec. 2014.

[22] Y. Dhungana, N. Rajatheva, and C. Tellambura, "Performance analysis of antenna correlation on LMS-based dual-hop AF MIMO systems," *IEEE Trans. Veh. Technol.*, vol. 61, no. 8, pp. 3590–3602, Oct. 2012.

[23] M. R. Bhatnagar, "Performance evaluation of decode-and-forward satellite relaying," *IEEE Trans. Veh. Technol.*, vol. 64, no. 10, pp. 4827–4833, Oct. 2015.

[24] M. K. Arti and S. K. Jindal, "OSTBC transmission in shadowed-Rician land mobile satellite links," *IEEE Trans. Veh. Technol.*, vol. 65, no. 7, pp. 5771–5777, Jul. 2016.

[25] Y. Dhungana and N. Rajatheva, "Analysis of LMS based dual hop MIMO systems with beamforming," in *Proc. IEEE Int. Conf. Commun. (ICC)*, Kyoto, Japan, Jun. 2011, pp. 1–6.

[26] S. Gong, D. Wei, X. Xue, and M. Y. Chen, "Study on the channel model and BER performance of single-polarization satellite-earth MIMO communication systems at Ka band," *IEEE Trans. Antennas Propag.*, vol. 62, no. 10, pp. 5282–5297, Oct. 2014.

[27] N. I. Miridakis, D. D. Vergados, and A. Michalas, "Dual-hop communication over a satellite relay and shadowed Rician channels," *IEEE Trans. Veh. Technol.*, vol. 64, no. 9, pp. 4031–4040, Sep. 2015.

[28] K. An *et al.*, "Performance analysis of multi-antenna hybrid satellite-terrestrial relay networks in the presence of interference," *IEEE Trans. Commun.*, vol. 63, no. 11, pp. 4390–4404, Nov. 2015.

[29] X. Artiga, J. Nunez-Martinez, A. Perez-Neira, G. J. L. Vela, J. M. F. Garcia, and G. Ziaragkas, "Terrestrial-satellite integration in dynamic 5G backhaul networks," in *Proc. 8th Adv. Satellite Multimedia Syst. Conf., 14th Signal Process. Space Commun. Workshop (ASMS/SPSC)*, Palma de Mallorca, Spain, Sep. 2016, pp. 1–6.

[30] Y. Ruan, Y. Li, C.-X. Wang, R. Zhang, and H. Zhang, "Outage performance of integrated satellite-terrestrial networks with hybrid CCI," *IEEE Commun. Lett.*, vol. 21, no. 7, pp. 1545–1548, Jul. 2017.

[31] P. K. Sharma, P. K. Upadhyay, D. B. da Costa, P. S. Bithas, and A. G. Kanatas, "Performance analysis of overlay spectrum sharing in hybrid satellite-terrestrial systems with secondary network selection," *IEEE Trans. Wireless Commun.*, vol. 16, no. 10, pp. 6586–6601, Oct. 2017.

[32] H. Baek and J. Lim, "Spectrum sharing for coexistence of fixed satellite services and frequency hopping tactical data link," *IEEE J. Sel. Areas Commun.*, vol. 34, no. 10, pp. 2642–2649, Oct. 2016.

[33] X. Yan, H. Xiao, C.-X. Wang, and K. An, "Outage performance of NOMA-based hybrid satellite-terrestrial relay networks," *IEEE Wireless Commun. Lett.*, to be published, doi: 10.1109/LWC.2018.2793916.

[34] T. Akiyoshi, E. Okamoto, H. Tsuji, and A. Miura, "Performance improvement of satellite/terrestrial integrated mobile communication system using unmanned aerial vehicle cooperative communications," in *Proc. Int. Conf. Inf. Netw. (ICOIN)*, Da Nang, Vietnam, Jan. 2017, pp. 417–422.

[35] H. Skinnemoen, "UAV & satellite communications live mission-critical visual data," in *Proc. IEEE Int. Conf. Aerosp. Electron. Remote Sens. Technol. (ICARES)*, Yogyakarta, Indonesia, Nov. 2014, pp. 12–19.

[36] A. Abdi *et al.* "A new simple model for land mobile Satellite channels: First and second order statistics," *IEEE Trans. Wireless Commun.*, vol. 2, no. 3, pp. 519–528, May 2003.

[37] C. Loo, "A statistical model for a land mobile satellite link," *IEEE Trans. Veh. Technol.*, vol. 34, no. 3, pp. 122–127, Aug. 1985.

[38] M. K. Arti, "Channel estimation and detection in satellite communication systems," *IEEE Trans. Veh. Technol.*, vol. 65, no. 12, pp. 10173–10179, Dec. 2016.

[39] H. A. Suraweera, H. K. Garg, and A. Nallanathan, "Performance analysis of two hop amplify-and-forward systems with interference at the relay," *IEEE Commun. Lett.*, vol. 14, no. 8, pp. 692–694, Aug. 2010.

[40] M. K. Simon and M.-S. Alouini, *Digital Communication Over Fading Channels: A Unified Approach to Performance Analysis*. Hoboken, NJ, USA: Wiley, 2000.

[41] M. Li, M. Lin, W. P. Zhu, Y. Huang, A. Nallanathan, and Q. Yu, "Performance analysis of MIMO MRC systems with feedback delay and channel estimation error," *IEEE Trans. Veh. Technol.*, vol. 65, no. 2, pp. 707–717, Feb. 2016.
[42] J. Tang and X. Zhang, "Transmit selection diversity with maximal-ratio combining for multicarrier DS-CDMA wireless networks over Nakagami-*m* fading channels," *IEEE J. Sel. Areas Commun.*, vol. 24, no. 1, pp. 104–112, Jan. 2006.
[43] G. Alfano and A. D. Maio, "Sum of squared shadowed-Rice random variables and its application to communication systems performance prediction," *IEEE Trans. Wireless Commun.*, vol. 6, no. 10, pp. 3540–3545, Oct. 2007.
[44] D. B. da Costa, H. Ding, and J. Ge, "Interference-limited relaying transmissions in dual-hop cooperative networks over Nakagami-*m* fading," *IEEE Commun. Lett.*, vol. 15, no. 5, pp. 503–505, May 2011.
[45] D. B. da Costa and M. D. Yacoub, "Outage performance of two hop AF relaying systems with co-channel interferers over Nakagami-*m* fading," *IEEE Commun. Lett.*, vol. 15, no. 9, pp. 980–982, Sep. 2011.
[46] J. C. S. S. Filho and M. D. Yacoub, "Nakagami-*m* approximation to the sum of M non-identical independent Nakagami-*m* variates," *Electron. Lett.*, vol. 40, no. 15, pp. 951–952, Jul. 2004.
[47] A. M. Mathai and R. K. Saxena, *The H-Function With Applications in Statistics and Other Disciplines*. Hoboken, NJ, USA: Wiley, 1978.
[48] I. Trigui, S. Affes, and A. Stéphenne, "Ergodic capacity of two-hop multiple antenna AF systems with co-channel interference," *IEEE Wireless Commun. Lett.*, vol. 4, no. 1, pp. 26–29, Feb. 2015.
[49] I. S. Gradshteyn and I. M. Ryzhik, *Tables of Integrals, Series and Products*, 6th ed. New York, NY, USA: Academic, 2000.
[50] R. P. Agrawal, "On certain transformation formulae and Meijer's G-function of two variables," *Indian J. Pure Appl. Math.*, vol. 1, no. 4, pp. 537–551, 1970.
[51] V. S. Adamchik and O. I. Marichev, "The algorithm for calculating integrals of hypergeometric type functions and its realization in REDUCE system," in *Proc. Int. Symp. Symbolic Algebraic Comput. (ISSAC)*, Tokyo, Japan, Aug. 1990, pp. 212–224.
[52] I. S. Ansari, S. Al-Ahmadi, F. Yilmaz, M.-S. Alouini, and H. Yanikomeroglu, "A new formula for the BER of binary modulations with dual-branch selection over generalized-K Composite fading channels," *IEEE Trans. Commun.*, vol. 59, no. 10, pp. 2654–2658, Oct. 2011.

VINAY BANKEY (S'16) received the B.E. degree in electronics and communication engineering from Rajiv Gandhi Proudyogiki Vishwavidyalaya, Bhopal, India, in 2012, and the M.Tech. degree in communication system engineering from the Visvesvaraya National Institute of Technology, Nagpur, India, in 2014. He is currently pursuing the Ph.D. degree with the Wireless Communications Research Group, IIT Indore, Indore, India. His research interests include hybrid satellite-terrestrial systems, cooperative relaying, multiple-input multiple-output communication systems, and physical-layer security.

PRABHAT K. UPADHYAY (S'09–M'13–SM'16) received the Ph.D. degree in electrical engineering from IIT Delhi, New Delhi, India, in 2011. He was a Lecturer with the Department of Electronics and Communication Engineering, Birla Institute of Technology Mesra, Ranchi. He joined in electrical engineering with IIT Indore as an Assistant Professor in 2012, where he has been an Associate Professor since 2017. He has also been leading various research projects with the Wireless Communications Research Group, IIT Indore. He has numerous publications in peer-reviewed journals and conferences, and has authored a book and three book chapters. His main research interests include wireless relaying techniques, cooperative communications, MIMO signal processing, hybrid satellite-terrestrial systems, cognitive radio, and molecular communications. He is a member of the IEEE Communications Society, the IEEE Vehicular Technology Society, and a Life Member of the Institution of Electronics and Telecommunication Engineers. He was a co-recipient of the Best Paper Awards at the International Conference on Advanced Communication Technologies and Networking, Marrakech, Morocco, in 2018. He has been awarded the Sir Visvesvaraya Young Faculty Research Fellowship under Ministry of Electronics and Information Technology, Government of India. He is currently serving as an Associate Editor of the IEEE ACCESS and as a Guest Editor of Special Issue on Energy-Harvesting Cognitive Radio Networks in the IEEE TRANSACTIONS ON COGNITIVE COMMUNICATIONS AND NETWORKING. He is involved in Technical Program Committee of several premier conferences.

DANIEL BENEVIDES DA COSTA (S'04–M'08–SM'14) was born in Fortaleza, Ceará, Brazil, in 1981. He received the B.Sc. degree in telecommunications from the Military Institute of Engineering, Rio de Janeiro, Brazil, in 2003, and the M.Sc. and Ph.D. degrees in electrical engineering, with a focus on telecommunications, from the University of Campinas, SP, Brazil, in 2006 and 2008, respectively. From 2008 to 2009, he was a Post-Doctoral Research Fellow with INRS-EMT, University of Quebec, Montreal, QC, Canada. Since 2010, he has been with the Federal University of Ceará, where he is currently an Associate Professor. From 2012 to 2017, he was a Member of the Advisory Board of the Ceará Council of Scientific and Technological Development, with a focus on telecommunications. He is a member of the IEEE Communications Society and the IEEE Vehicular Technology Society. He was a recipient of four conference paper awards. His Ph.D. thesis was awarded the Best Ph.D. Thesis in electrical engineering by the Brazilian Ministry of Education at the 2009 CAPES Thesis Contest. He is the Chair of the Special Interest Group on Energy-Harvesting Cognitive Radio Networks in the IEEE Cognitive Networks Technical Committee. He received the Exemplary Reviewer Certificate of the IEEE WIRELESS COMMUNICATIONS LETTERS in 2013, the Exemplary Reviewer Certificate of the IEEE COMMUNICATIONS LETTERS in 2016 and 2017, the Certificate of Appreciation of Top Associate Editor for outstanding contributions to the IEEE TRANSACTIONS ON VEHICULAR TECHNOLOGY, in 2013, 2015, and 2016, respectively, the Exemplary Editor Award of the IEEE COMMUNICATIONS LETTERS in 2016, and the Outstanding Editor Award of the IEEE ACCESS in 2017. He is a Distinguished Lecturer of the IEEE Vehicular Technology Society. He is currently Editor of the IEEE COMMUNICATIONS SURVEYS AND TUTORIALS, the IEEE ACCESS, the IEEE TRANSACTIONS ON COMMUNICATIONS, the IEEE TRANSACTIONS ON VEHICULAR TECHNOLOGY, and *EURASIP Journal on Wireless Communications and Networking*. He has also served as Associate Technical Editor of the IEEE *Communications Magazine*. From 2012 to 2017, he was Editor of the IEEE COMMUNICATIONS LETTERS. He has served as Area Editor of *KSII Transactions on Internet and Information Systems* and as a Guest Editor of several Journal Special Issues. He has been involved on the organizing committee of several conferences. He is currently the Latin American Chapters Coordinator of the IEEE Vehicular Technology Society. Also, he acts as a Scientific Consultant of the National Council of Scientific and Technological Development, Brazil, and also a Productivity Research Fellow of CNPq.

PETROS S. BITHAS (S'04–M'09) received the B.S. degree in electrical engineering and the Ph.D. degree in wireless communication systems from the Department of Electrical and Computer Engineering, University of Patras, Greece, in 2003 and 2009, respectively. From 2004 to 2009, he was a Research Assistant with the Institute for Space Applications and Remote Sensing, National Observatory of Athens (NOA), Greece. Since 2009, he has been with the Department of Electronics Engineering, Technological Educational Institute of Piraeus, as a Lab Instructor. From 2010 to 2013, he was a Post-Doctoral Researcher with the Department of Digital Systems, University of Piraeus, and from 2013 to 2015, he was with the Institute for Astronomy, Astrophysics, Space Applications and Remote Sensing, NOA. Since 2015, he has been a Post-Doctoral Researcher with the Department of Digital Systems, University of Piraeus. He has published 30 articles in international scientific journals and 33 articles in the proceedings of international conferences. His current research interests include the stochastic modeling of wireless communication channels, performance analysis of mobile communications systems, cooperative diversity reception systems, cognitive relaying techniques, and distributed MIMO techniques. He has served as a Project Evaluator for the General Secretariat for Research and Technology in 2010 and the Czech Science Foundation in 2011, 2012, and 2014–2017. He has been selected as an Exemplary Reviewer of the IEEE COMMUNICATIONS LETTERS in 2010, while he was also a co-recipient of Best Paper Awards at the IEEE International Symposium on Signal Processing and Information Technology in 2013. He serves on the Editorial Board of the *International Journal of Electronics and Communications* (Elsevier).

ATHANASIOS (THANASIS) G. KANATAS (S'90–M'93–SM'02) received the Diploma degree in electrical engineering from the National Technical University of Athens (NTUA), Greece, in 1991, the M.Sc. degree in satellite communication engineering from the University of Surrey, Surrey, U.K., in 1992, and the Ph.D. degree in mobile satellite communications from NTUA in 1997. From 1993 to 1994, he was with the National Documentation Center, National Research Institute. In 1995, he joined Spacetec Ltd., as a Technical Project Manager for the VISA/EMEA VSAT Project in Greece. In 1996, he joined the Mobile Radio-Communications Laboratory as a Research Associate. From 1999 to 2002, he was with the Institute of Communication and Computer Systems responsible for the technical management of various research projects. In 2000, he became a member of the Board of Directors of OTESAT S.A. In 2002, he joined the University of Piraeus, Greece, as an Assistant Professor, where he is currently a Professor with the Department of Digital Systems and the Dean of the School of Information and Communication Technologies. He has published over 150 papers in international journals and international conference proceedings. He is the author of six books in the field of wireless and satellite communications in Greek and/or English language. He has been a technical manager of several European and national research and development projects. His current research interests include the development of new digital techniques for wireless and satellite communications systems, channel characterization, simulation, and modeling for mobile, mobile satellite, and future wireless communication systems, antenna selection and RF preprocessing techniques, new transmission schemes for MIMO systems, V2V communications, and energy efficient techniques for wireless sensor networks. In 1999, he was an Elected Chairman of the Communications Society of the Greek Section of the IEEE.

UGO SILVA DIAS (S'04–M'08–SM'18) was born in Belém, Brazil, in 1981. He received the B.Sc. degree in electrical engineering from the Federal University of Pará, Brazil, in 2004, and the M.Sc. and Ph.D. degrees in electrical engineering (major in telecommunications) from the University of Campinas, Brazil, in 2006 and 2010, respectively. Since 2010, he has been an Assistant Professor with the University of Brasília, Brazil. Besides the academic experiences, he also worked in several companies in the ICT industry. He is currently a Faculty Member with the MWSL Lab, Department of Electrical Engineering, and the Latitude Lab. His main research interests include fading channels, field measurements, coexistence of future wireless networks, cognitive radio, and wireless technologies in general. He is a member of the IEEE Communications Society, the Brazilian Telecommunications Society, and the Brazilian Communications Committee. He was a recipient of four conference paper awards and one award from IEEE R9 for the first place in the IEEE R9 Success Story Contest–ComSoc Student Chapter 2017. He has been involved on the organizing committee of several conferences. He is currently the Chair of the IEEE ComSoc CN Brazil Chapter, an Advisor of the IEEE ComSoc UnB Student Branch Chapter, and a VP of the Brazilian Telecommunications Society. He is currently an Editor of the *IET Electronics Letters* and *ACTA Press–Communications*.